

This article was downloaded by:

On: 25 January 2011

Access details: *Access Details: Free Access*

Publisher *Taylor & Francis*

Informa Ltd Registered in England and Wales Registered Number: 1072954 Registered office: Mortimer House, 37-41 Mortimer Street, London W1T 3JH, UK



Journal of Wood Chemistry and Technology

Publication details, including instructions for authors and subscription information:

<http://www.informaworld.com/smpp/title~content=t713597282>

A Model for Chlorine Dioxide Delignification of Chemical Pulp

Ville Tarvo^a; Tuula Lehtimaa^b; Susanna Kuitunen^a; Ville Alopaeus^a; Tapani Vuorinen^b; Juhani Aittamaa^a

^a Department of Biotechnology and Chemical Technology, TKK, Espoo, Finland ^b Department of Forest Products Technology, TKK, Espoo, Finland

Online publication date: 15 September 2010

To cite this Article Tarvo, Ville , Lehtimaa, Tuula , Kuitunen, Susanna , Alopaeus, Ville , Vuorinen, Tapani and Aittamaa, Juhani(2010) 'A Model for Chlorine Dioxide Delignification of Chemical Pulp', *Journal of Wood Chemistry and Technology*, 30: 3, 230 – 268

To link to this Article: DOI: 10.1080/02773810903461476

URL: <http://dx.doi.org/10.1080/02773810903461476>

PLEASE SCROLL DOWN FOR ARTICLE

Full terms and conditions of use: <http://www.informaworld.com/terms-and-conditions-of-access.pdf>

This article may be used for research, teaching and private study purposes. Any substantial or systematic reproduction, re-distribution, re-selling, loan or sub-licensing, systematic supply or distribution in any form to anyone is expressly forbidden.

The publisher does not give any warranty express or implied or make any representation that the contents will be complete or accurate or up to date. The accuracy of any instructions, formulae and drug doses should be independently verified with primary sources. The publisher shall not be liable for any loss, actions, claims, proceedings, demand or costs or damages whatsoever or howsoever caused arising directly or indirectly in connection with or arising out of the use of this material.

A Model for Chlorine Dioxide Delignification of Chemical Pulp

Ville Tarvo,¹ Tuula Lehtimaa,² Susanna Kuitunen,¹ Ville Alopaeus,¹
Tapani Vuorinen,² and Juhani Aittamaa¹

¹Department of Biotechnology and Chemical Technology, TKK, Espoo, Finland

²Department of Forest Products Technology, TKK, Espoo, Finland

Abstract: A phenomenon based model for chlorine dioxide delignification of chemical pulp is introduced. The pulp suspension environment is modeled using the concept of two liquid phases, one inside and the other external to the fiber wall. Physico-chemical processes taking place during delignification are implemented with thermodynamic, mass transfer and reaction kinetic models. A broad library of chemical reactions is introduced. Inclusion of each reaction is justified. The model response is tested against experimental laboratory delignification results (o-delignified birch pulp). The experimental data consists of kappa number, hexenuronic acid, inorganic oxy-chlorine compound, and organochlorine (AOX, OX) measurements at several time points during five delignification experiments. The model predictions are mainly in good agreement with the experimental results. The predictions regarding hypochlorous acid driven processes (HexA removal, organochlorine formation, chlorite and chlorate concentration) are somewhat incoherent, indicating that knowledge regarding the intermediately formed hypochlorous acid is presently insufficient.

Keywords: Chlorine dioxide delignification, bleaching, modeling, reaction kinetics

INTRODUCTION

Chlorine dioxide (ClO_2) is one of the primary bleaching agents applied in chemical pulp bleaching. It is used both in the delignifying (prebleaching) stage (D0) and in the brightening stages (D1 and D2). Despite the wide use and several decades of active research, many aspects regarding the chemistry

Gratitude is shown for all parties of the ABLE and VIP projects: the researchers for input in model development; the Technology Development Agency of Finland (TEKES) and participating companies for financial support. The Graduate School in Chemical Engineering is acknowledged for funding.

Address correspondence to Ville Tarvo, Department of Biotechnology and Chemical Technology, P.O. Box 6100, TKK, Espoo FI-02015, Finland. E-mail: ville.tarvo@tkk.fi

of chlorine dioxide bleaching are still not well understood. Part of the related research has involved models for mimicking and predicting the behavior of the real bleaching system. The presently available models typically employ one or two empirical correlations to predict the kinetics in kappa number development.^[1-5] An extended version by Mortha et al.^[6] predicts the development of pH and the concentration of certain inorganic oxy-chlorine species in parallel with kappa number. Correlations are simple and fast to use. They are beneficial in forming a gross linkage between the key process variables and the delignification/bleaching result. As a downside, the correlation parameters rarely have physical meaning and the parameter values are typically tied to the experimental setup (pulp type, conditions, apparatus, etc.). Consequently, the models have little applicability outside the validation data. Another limitation of the kappa correlations is that the maximum delignification result (highest attainable kappa number drop) is required as an input parameter. In many cases the research objective would be to find ways to exceed the apparent maximum performance. Gu and Edwards^[7] have established a model based on chemical reactions between chlorine dioxide/chlorine and various organic compounds in pulp and in the surrounding liquor. Some inorganic reactions are also incorporated. This approach is encouraging, although the set of reactions is brief and the pulp suspension properties (two liquid phases, Donnan phenomenon) and diffusional aspects are disregarded.

Modeling and simulation tools are widely utilized in research related to chemical and petrochemical industries. The models used in these disciplines represent phenomenon based models (i.e., they rely on fundamental phenomena such as thermodynamics, chemical reactions, mass transfer, and fluid dynamics). The benefit of phenomenon models is that they are valid regardless of the reaction environment. The same models and parameters apply independent of the size or shape of an apparatus, or any other external constraint. Consequently, the models have broad applicability in laboratory research, in process scale-up, as well as in mill-scale investigations. This report introduces a phenomenon based model for chlorine dioxide delignification of chemical pulp. The concept of two liquid phases is applied (one inside the fiber wall, the other external to fibers), the dissociation of fiber wall and dissolved acids is incorporated, the uneven distribution of ions between the two liquids is taken into account, and mass transfer and reaction kinetics are modeled separately. Documented thermochemical and reaction rate parameters are exploited as much as possible. The unknown parameters are obtained through comparison of model predictions against experimental laboratory scale results (o-delignified birch pulp).

THE CHLORINE DIOXIDE DELIGNIFICATION MODEL

The Model for Pulp Suspension

The main constituents in pulp suspensions are wood fibers, water, and chemicals dissolved in water. The fibers are modeled as hollow cylinders. When

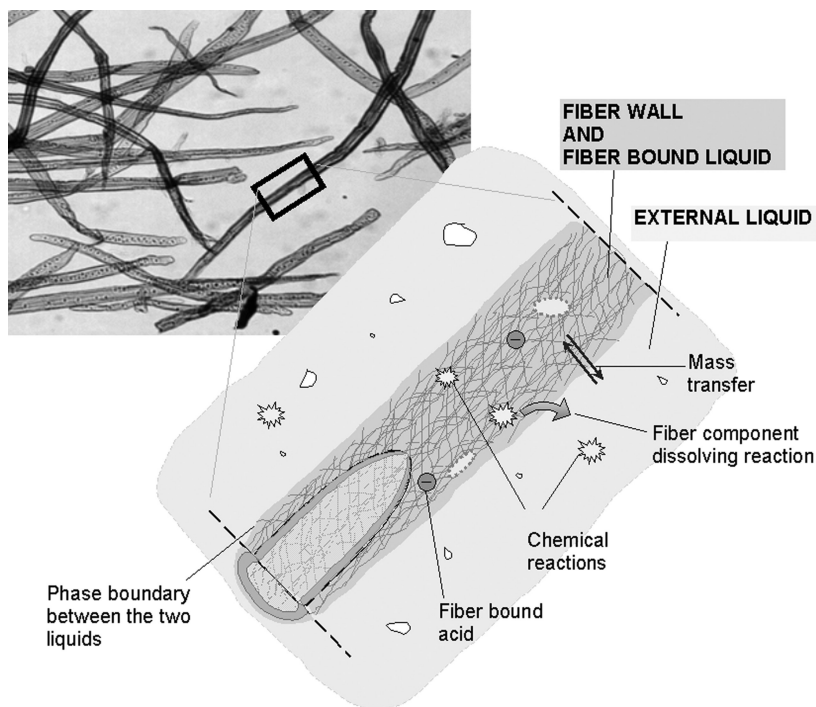


Figure 1. A schematic picture of the pulp delignification model.

suspended into aqueous medium, the fiber wall absorbs liquid. The stagnant liquid inside the fiber wall is considered separate from the bulk liquid and is referred to as the fiber bound liquid. The bulk liquid, both outside the cylindrical fibers and inside the lumen, is referred to as the external liquid. The lumen liquid is assumed to be in free contact with the liquid outside the fibers through pits in the fiber wall. A schematic representation of the system is shown in Figure 1. The volume of the fiber bound liquid is defined via the fiber saturation point (FSP). Compounds in the fiber bound liquid may react with each other or with the solid (immobile) fiber wall compounds. The solid fiber wall compounds are assumed to be uniformly distributed in the cell wall and fully accessible to react with the fiber bound liquid compounds. Chlorine dioxide is known to be a very selective lignin oxidant, reacting much faster with lignin than with pulp carbohydrates.^[8] Thus, cellulose and hemicelluloses, except for hexenuronic acids (HexA), are assumed to be inert. Lignin is modeled with monomeric pseudo-compounds. This simplification enables efficient incorporation of the chemical characteristics and reactions of various lignin structures, although ensuing compromises in modeling the macromolecular features of lignin. Syringyl and guaiacyl lignin units are distinguished with regard to molar weight; their reaction paths and kinetics are assumed to be equal. Macromolecular

aspects of lignin are considered only in modeling lignin dissolution. Oxidative reactions break down the lignin structures and create hydrophilic groups. Both actions promote lignin solubility in aqueous media.^[9] Lignin dissolution is modeled as a transfer process of compounds from the insoluble fiber wall into the fiber bound liquid.

Acidic groups in carbohydrates and in lignin contribute to the electrostatic equilibrium of the fiber bound liquid. This causes an uneven distribution of mobile ions between the two liquid phases. The Donnan theory^[10–14] is used to define the distribution of ions. Detailed modeling principles regarding mass transfer, protolysis equilibria, and Donnan equilibrium are given in a previous paper.^[15] Heat losses and heats of reaction are assumed to be negligible.

Reactions between ClO₂ and Lignin

A full list of all incorporated chemical reactions and rate parameters is given in the Appendix. The list is not assumed to contain all conceivable reactions that may take place during delignification, but is put out as a simplified model for the essential chemical reactions. The list may be modified and extended as knowledge regarding the reaction paths and intermediate structures increases.

Phenyl propane units are used to model unreacted residual lignin, either phenolic or non-phenolic. The reaction between chlorine dioxide and the unreacted (primary) lignin proceeds via three parallel paths (Figure 2, reactions 1–12 in the Appendix). Path (A) produces a quinone, path (B) produces a muconic acid ester/the corresponding lactone, and path (C) produces a reactive intermediate. The quinone pseudo-compound accounts for both *para*- and *ortho*-quinones. Quinones^[16–21] and muconic acids^[16–19,21–24] have both been identified as direct oxidation products of lignin model compounds. Indirect evidence of quinone formation has also been obtained from pulps^[25] and isolated residual lignins.^[26] Based on the fact that quinones and muconic acid esters are found in D-stage pulps and lignins, both structures are assumed to be stable toward further oxidation. Path (C) accounts for experimental findings that a significant part of the lignin is degraded beyond the level of quinones and muconic acids^[18,19,23,24] and that chlorine dioxide is consumed more extensively than required to reach the muconic acid/quinone level.^[27] The structure of the reactive intermediate is unknown and it is depicted here as a non-esterified muconic acid merely to indicate the level of oxidation. The relative importance of reaction paths A–C depends on the detailed structure of the lignin substrate.^[18, 23, 24] In the model, the reaction paths are assumed to proceed in a 1:1:2 ratio (A:B:C), resembling the proportions reported for vanillyl alcohol.^[18]

The reactions depicted in Figure 2 concern both phenolic and non-phenolic lignin. The reaction kinetics for phenolic lignin is defined according to the oxidation rate of 2-methoxyphenol ($k_{\text{dissociated}} = 1 \cdot 10^9 \text{ M}^{-1} \text{ s}^{-1}$, $k_{\text{undissociated}} = 1 \cdot 10^3 \text{ M}^{-1} \text{ s}^{-1}$).^[28] The rate parameters reported for other phenols are of similar

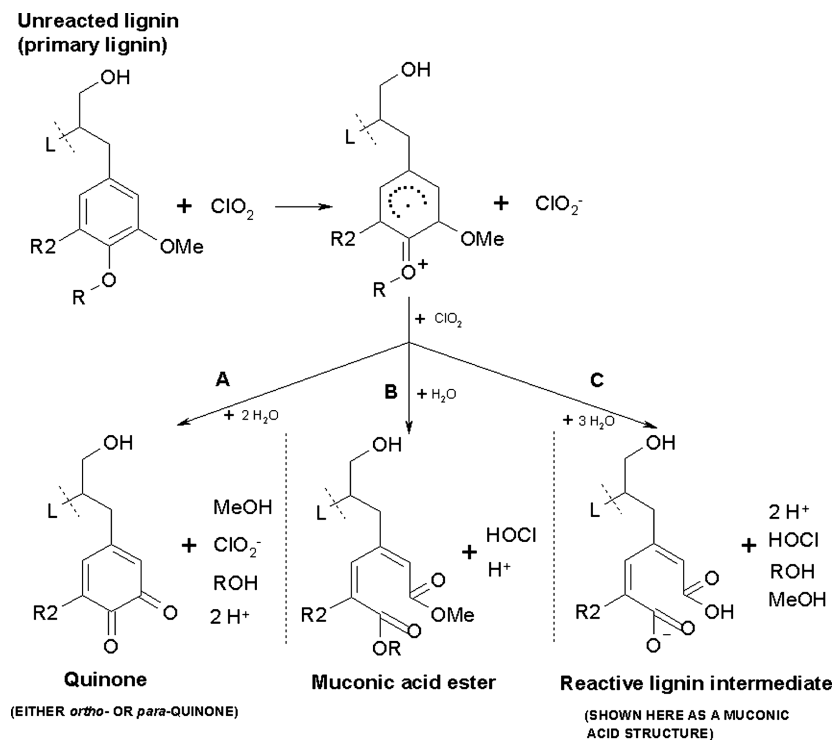


Figure 2. The oxidation of primary lignin by chlorine dioxide. ($\text{R}_2 = \text{H}$ for guaiacyl lignin, $\text{R}_2 = \text{OMe}$ for syringyl lignin; $\text{R} = \text{H}$ for phenolic lignin, $\text{R} = -\text{Lignin}$ for non-phenolic lignin).

magnitude.^[20,28] The rate of non-phenolic lignin oxidation is adopted from Brage et al.^[19] Chlorine substituents are believed to cause steric hindrance and retard the oxidative cleavage of ether bonds.^[29] Hence, chlorine substituted structures are assumed to be oxidized an order of magnitude slower than the unchlorinated counterparts. This principle applies for all lignin oxidation reactions.

The reactive intermediate produced from primary lignin through path C (Figure 2) is assumed to yield maleic acid in a reaction with chlorine dioxide.^[23,24] The overall stoichiometry for guaiacyl type lignin is given in Figure 3 (reactions 13 and 14 in the Appendix). Experimental information regarding the type and ratio of the inorganic products is not available. The reaction is assumed to produce chlorite (ClO_2^-) and hypochlorous acid (HOCl) in a 1:1 stoichiometry. This assumption is based on the fact that the suspension pH in our experiments was between 2.7 and 4.2 for the majority of the reaction time (1–30 min), and roughly 50% of the initial ClO_2 is reported to be converted

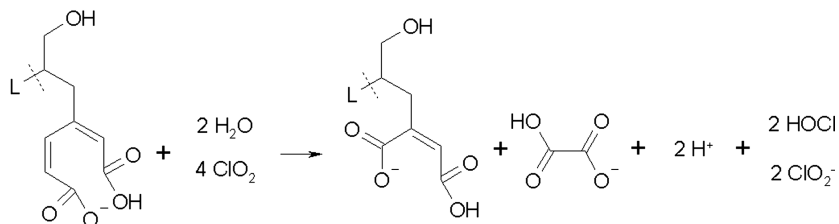
Reactive lignin intermediate

Figure 3. The stoichiometry in chlorine dioxide oxidation of the reactive lignin intermediate (depicted as a free muconic acid) into maleic acid.

to HOCl during delignification experiments at pH 2.5–4.^[30–32] Maleic acid is assumed to be oxidized further to produce a highly fractionated, fully saturated lignin derivative, referred to as C5-acid (Figure 4, reactions 15 and 16 in the Appendix). The rate parameters for reactions (13–16) are obtained through regression against the experimental data. The regression is controlled so that the oxidation susceptibilities (reaction kinetics) of the lignin pseudo-compounds decrease with the extent of oxidation. All lignin reactions are assumed to proceed similarly in the fiber wall and in the liquor, that is, the same reaction routes and kinetics apply for the lignin pseudo-components in liquor (dissolved) or in the fiber wall (insoluble).

Reactions between HOCl/Cl₂ and Lignin

Hypochlorous acid is one of the key in-situ formed chlorine species in ClO₂ delignification. It is mainly formed by reduction of chlorine dioxide in reactions with organic substrates (Figures 2–4), but also in reactions involving only inorganic oxy-chlorine species (reactions 35, 36, 40). In the model, hypochlorous acid is assumed to chlorinate phenols^[33–35] (reaction 17) and generate phenolic

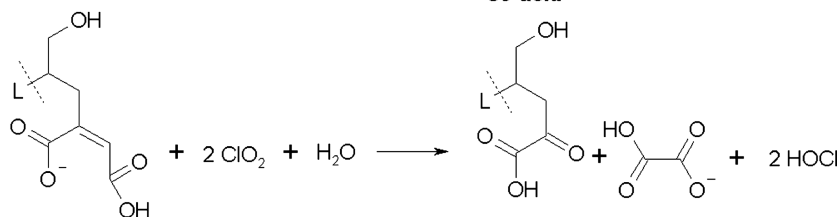
Maleic acid

Figure 4. Oxidation of maleic acid into C5-acid by ClO₂.

groups in lignin (reaction 18). The kinetics of phenolic lignin chlorination is defined according to experimental results reported for phenol ($k_{17,\text{dissociated}} = 10^4 \text{ M}^{-1}\text{s}^{-1}$, $k_{17,\text{undissociated}} = 0.1 \text{ M}^{-1}\text{s}^{-1}$).^[33,35] The chlorination reaction between etherified phenols and HOCl is reported to be slow ($k = 0.019 \text{ M}^{-1}\text{s}^{-1}$).^[35] Aromatic compounds without specific substituents are also known to react slowly with hypochlorous acid^[36] and hence the reaction between non-phenolic lignin and HOCl is assumed to be insignificant. The reaction that generates new phenolic groups (reaction 18) is incorporated based on implications from experimental work.^[37,38] The rate of the phenol generating reaction (reaction 18) is obtained from regression.

In acidic medium, hypochlorous acid and chloride ions form elemental chlorine in a reversible reaction^[39] (reactions 41, 42). Chlorine is known to both chlorinate (reactions 19–20) and oxidize (reactions 21–24) lignin.^[29] Chlorination experiments have indicated that the C₉-lignin units become monochlorinated almost instantaneously.^[40] Thus, we assume chlorination (reactions 19–20) to occur one order of magnitude faster than oxidation (reactions 21–24). The absolute values of the reaction rate parameters are obtained from regression. The chlorination reactions are assumed to yield only monochlorinated compounds.^[41] The chlorine substitution is assumed to occur at position 5 of the aromatic ring.^[42,43]

Lignin Dissolution

The macromolecular nature of lignin is taken into account in the dissolution reactions of lignin. The following principles were used in the lignin dissolution scheme: (i) dissolution is directly proportional to the extent of lignin fragmentation and accumulation of hydrophilic groups (carboxylic acids) and (ii) the dissolving entity (“lignin fragment”) is a sum of monomeric units. An example of a lignin dissolving reaction and the dissolution rate equation is given in Figure 5. The complete list of dissolution reactions is given in the Appendix (reactions 66–101). The oxidative reactions of ClO₂ and other oxychlorine species increase fragmentation and hydrophilicity of residual lignin and force some of the lignin to dissolve. The hydrophilic lignin derivatives are assumed to be attached to other lignin units and hence to force some unreacted lignin also to dissolve. The rate of each dissolution reaction is proportional both to the concentration of the fragmented/hydrophilic lignin derivative and the unreacted lignin unit. The more extensively degraded lignin derivatives (C5-acid > maleic acid > muconic acid) are assumed to dissolve a larger fraction of unreacted structures, and vice versa. Guidelines for choosing the dissolution stoichiometry (the ratio of fragmented/hydrophilic lignin derivatives to the primary lignin units) were adopted from studies dealing with dissolved D0-stage lignin (Table 1). The reported properties must be viewed with reserve, since they often concern “high molecular weight material” (HMW material) rather than

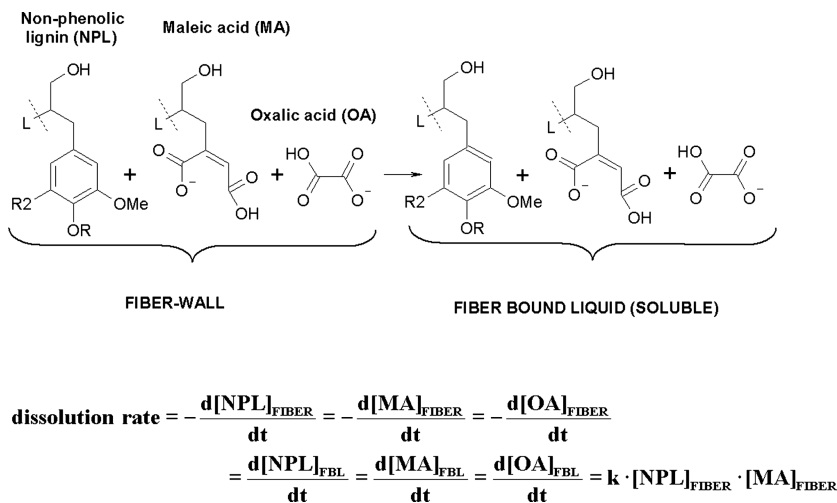


Figure 5. An example of a lignin dissolution reaction (reaction 79 in the Appendix).

pure dissolved lignin. The HMW material from D0-stage (HW) is reported to contain 13% of carbohydrates, mainly xylan.^[44] The C:O ratios are consistently around 1.5, independent of a preceding O-stage or wood species (Table 1). The reported carboxyl group contents are more divergent. The dissolving lignin fragments in our model have C:O ratios between 1.3 and 2.2. The model fragment carboxyl group content varies between 5 and 11 mmol/g, which is in line with the experimental values. The kinetic parameters for the lignin dissolution reactions are obtained from regression. All reactions are assumed to have the

Table 1. Properties of high molecular weight (HMW) material dissolved during chlorine dioxide delignification

aSW/HW	Oxygen delignified	bC/O	Carboxyl groups		Reference
			Quantity (mmol/g)	Determination method (method of titration)	
SW	no	1.6	3.1–4.5	potentiometric	[45]
SW	no	1.2	8.7	potentiometric	[46]
			10.5	conductometric	
HW	yes	1.5	3.1	conductometric	[44]

aHW = hardwood, SW = softwood.

bC/O = carbon to oxygen ratio.

same rate. The principle of higher lignin degradation and hydrophilicity leading to more extensive dissolution is achieved through differences in dissolution stoichiometry.

Hexenuronic Acid Reactions

Experimental work has shown that chlorine dioxide itself does not react effectively with hexenuronic acid.^[47] The active HexA degrading species are assumed to be hypochlorous acid and chlorine.^[47,48] We adopt this theory and implement reactions (25–32), which yield tetraric acid, pentaric acid, 2-chloro-2-deoxypentaric acid, and 3-deoxy-3,3-dichloro-2-oxohexaric acid as the final products.^[49–52] The reaction paths involving elemental chlorine (reactions 26,28) yield chlorinated products. Hence, lower pH increases the proportion of chlorinated degradation products, and vice versa. The correlation between pH and chlorinated HexA products has been observed in experimental work.^[52] The rate coefficients for the HexA degrading reactions are obtained from regression.

Extractives Reactions

Chlorine dioxide reacts readily with unsaturated sterols and fatty acids.^[53] Both reactions yield unchlorinated products.^[53,54] The contribution of extractives has been reported to be small on both OX and AOX formation in chlorine dioxide delignification of birch kraft pulp.^[55] Hence, chlorination of extractives by chlorine or hypochlorous acid was omitted. Reactions (33) and (34) are incorporated to account for the oxidation of these two extractive species. Both sitosterol and unsaturated fatty acids are reported to be removed to a very high extent during ClO₂ delignification.^[54] Hence, the rate coefficients are set to a high value ($k_{33} = k_{34} = 10 \text{ M}^{-1}\text{s}^{-1}$) reassuring rapid depletion.

Inorganic Oxy-Chlorine Reactions

As presented earlier (Figures 2–4), the primary reduction products of chlorine dioxide in delignification are chlorite ion and hypochlorous acid.^[17–19,30] Both compounds are known to react further in numerous reactions yielding various oxy- and organochlorine species as well as chloride ion (Cl⁻).^[30] The fully inorganic part of these reactions is thoroughly discussed in our previous work.^[56–58] Reactions (35–49) and the rate parameters are adopted from these papers.

Chlorine dioxide decomposition is known to be very slow in acidic solutions^[59–61] and delignification reactions are expected to consume chlorine dioxide much faster than the decomposition reaction.^[61,62] Chlorine dioxide decomposition is thus omitted in this work.

Protolysis Reactions and Other Equilibrium Reactions

The protolysis coefficients of chlorous acid (HClO_2) and hypochlorous acid (reactions 50–51) are computed from thermochemical constants as described earlier.^[15] The equilibrium coefficients for iron(III) hydroxylation (reactions 52–55) are computed in a similar manner. This procedure takes into account the temperature dependency of the dissociation coefficients. Lignin related phenols generally dissociate around pH 9–11.^[63,64] The pK_a -value reported for kraft lignin phenols (0.1 M NaCl), including the dissociation coefficient temperature dependency, is assigned for phenolic lignin (reaction 55).^[63] The value at 50°C is $\text{pK}_{a,\text{phenolic-lignin}} = 10.1$. Chlorine substituents are reported to decrease the pK_a -value of phenols by approximately one unit.^[28] Thus, chlorinated phenolic lignin is defined to have a one unit smaller pK_a -value than its unchlorinated equivalent (reaction 56). The value at 50°C the value is $\text{pK}_{a,\text{phenolic-lignin-Cl}} = 9.1$. The protolysis coefficients for maleic acid,^[65] oxalic acid,^[65] hexenuronic acid,^[66] and methyl-glucuronic acid^[66] (reactions 59, 60, 62–65) are defined according to the corresponding real compound values at 25°C. The temperature dependency of hexenuronic and methyl-glucuronic acid dissociation coefficients is estimated using the enthalpy of dissociation (–3 kJ/mol) reported for uronic acids in kraft pulp fibers.^[13]

MODEL VALIDATION

The model predictions were compared against kappa number, hexenuronic acid, inorganic oxy-chlorine compound, and organochlorine (AOX, OX) measurements at several time points during five delignification experiments. Chemical dose or temperature was varied in the experiments. The laboratory scale delignifications were done with Finnish oxygen-delignified birch kraft pulp. A complete description of the experimental procedures and results is given in two previous papers.^[67,68] The results are only revised here. The prediction/experimental comparison was straightforward with regards to the inorganic oxy-chlorine compounds, pH, and HexA content. The comparisons regarding lignin structures and organochlorine formation could not be done at molecular scale, as reliable analytical methods for detailed characterization of the residual and dissolved lignin were not available. Instead, the simulation results were converted into standardized bulk variables—kappa number, AOX, OX, and COD—to make the evaluation. The conversion principles are introduced below.

Kappa Number

The traditional 0.15 coefficient^[69] was used to convert the kappa number into residual lignin content (w-%), and vice versa. The hexenuronic acids were assumed to contribute with 0.086 kappa units/(mmol/kg) factor,^[70] as given in

Table 2. The oxidation equivalent values assigned for the lignin and extractive pseudo-compounds

Pseudo-compound	Reported KMnO ₄ oxidation equivalents ^[71–74]	The assigned oxidation equivalent value
Full aromatic ring (phenolic and non-phenolic lignin pseudo-compounds)	12–19.6	16
Quinone	6.8–12.5	10
Muconic acid	10.8–14.3	12
Maleic acid	10–11.7	11
Sterols	—	5.7
Unsaturated fatty acids	—	5.7

Eq. (1). Eq. (1) was solved for κ to compute the kappa number from the molecular scale composition (Eq. (2)). Lignin structures at various levels of oxidation were assumed to contribute variously in kappa number test. Thus, the lignin content, L , in Eq. (2) was handled as a proportioned summation term, as given in Eq. (3). The kappa contribution of the extractive components was incorporated through the summation term as well. Reported permanganate consumptions of lignin model compounds^[71–74] were used to define “oxidation equivalent” (OxEq) values for each lignin pseudo-compound (Table 2). The sterol and fatty acid pseudo-compounds were assigned the oxidation equivalent reported for an unconjugated double bond.^[71] The proportionality factor ($\text{OxEq}_i / \text{OxEq}_{\text{arom}}$) in Eq. (3) is unity for the unreacted lignin (full aromatic ring) and less than unity for the oxidized lignin pseudo-compounds and extractives. Compounds in the solid fiber wall and in the fiber bound liquid contribute to the computational kappa number. Compounds in the external liquid are omitted.

$$L = (\kappa - H \cdot 0.086) \cdot 0.15 \quad (1)$$

$$\kappa = L/0.15 + H \cdot 0.086 \quad (2)$$

$$L = 100\% \cdot \sum_i \left(\frac{\text{OxEq}_i}{\text{OxEq}_{\text{arom}}} \cdot M_{w,i} \cdot c_i \right) / 1000 \quad (3)$$

where

L = lignin content (weight%)

κ = kappa number

H = hexenuronic acid content (mmol/kg)

$M_{w,i}$ = molar weight of component i (g/mol)

c_i = component concentration (mol/kg fiber)

OxEq_i = oxidation equivalent value of component i

$\text{OxEq}_{\text{arom}}$ = oxidation equivalent value of full aromatic ring

Organochlorine Content (AOX, OX)

The AOX and OX values were computed by summing up the concentrations of all chlorine containing compounds in the external liquid (AOX) or in the solid fiber wall (OX), and proportioning the values to unit mass of dry fibers. 3-deoxy-3,3-dichloro-2-oxohexaric acid, the HexA degradation product from reaction 31, was assumed to contribute with a factor 2, as the molecule contains two chlorine atoms. The other AOX and OX compounds are monochlorinated and were assumed to contribute with a factor 1.

Chemical Oxygen Demand (COD)

The chemical oxygen demand (COD) was computed by determining the amount of oxygen required to oxidize the organic carbon and hydrogen in the external liquid phase compounds into water and carbon dioxide, respectively.

CONDUCTING THE SIMULATION

Simulation Progress

All simulations were conducted with Flowbat software.^[75] The composition of the raw materials (pulp and chlorine dioxide solution) was first defined. The lignin content (w-%) of the pulp was computed from Eqs. (1) and (3) using the experimental kappa number, HexA, and extractive contents. The obtained value was converted into mol/(kg fiber) using the molar mass of the unreacted lignin unit (1:1 ratio of syringyl and guaiacyl lignin,^[76] $M_w \approx 200$ g/mol). The reaction conditions (temperature, pressure) and suspension properties (FSP, pulp consistency) were then defined. The addition of chlorine dioxide was modeled as ideal mixing of the chlorine dioxide solution and the external liquid of the pulp. The addition of ClO_2 defined time point zero for the simulation. The progress of delignification was computed through reaction and mass transfer rate equations. Rate equations give the rate of change of moles per unit volume (mol/l-s) for each compound in each phase due to chemical reactions and mass transfer. Multiplication with the appropriate reaction volume (volume of each phase) yields the rate in mol/s. The resulting group of ordinary differential equations was solved using an ordinary differential equation solver.

Initial Values for the Simulations

The initial pulp and chlorine dioxide solution properties used in the simulations are given in Table 3. The values were mainly adopted from the experimental

Table 3. The initial pulp properties used in simulations

Variable	Value	Reference
Kappa number	12.5	[68]
Free phenol content	0.79 mol/kg lignin	[68]
HexA	55 mmol/ADkg	[68]
Methyl glucuronic acids	65 mmol/ADkg ^a	
Extractives	Sterols 0.45 g/ADkg ^b Fatty Acids 0.37 g/ADkg ^b	[80]
Pulp pH	8	[68]
Fiber saturation point	1.45 g water/g fiber ^b	[77]
pH of the ClO ₂ solution	2.2	
Fe	197 mmol/ODkg ^b	[78]
Pulp consistency after dilution and chemical addition	10%	[68]

^aSee text.

^bMeasured from Finnish oxygen delignified birch kraft pulp.

work.^[67,68] The pulp was assumed to be thoroughly washed, and thus to be free of dissolved organic compounds. The pulp was assumed to contain a small inorganic impurity ($I = 0.02 \text{ M NaHSO}_4$). The initial pulp pH was adjusted to 8 with NaOH. The experimental ClO₂ solution had been confirmed to be free of elemental chlorine.^[68] The ClO₂ solution acidity, pH = 2.2, was assumed to originate from sulfuric acid.

The simulation setup required information regarding the sterol and fatty acid contents, iron content, and methylglucuronic acid content of the pulp. These information were, unfortunately, not available from the pulp used in the experiments and the properties were estimated using literature data regarding similar pulps (Table 3). Finnish oxygen delignified birch kraft pulps are reported to contain 112–128 mmol/kg uronic acids.^[77–79] The total uronic acid content was assumed to consist of methylglucuronic and hexenuronic acids, and the methylglucuronic acid content was obtained by taking an average of the reported total contents and subtracting the experimental HexA amount.

Approximately 22% of the chlorine originally introduced as ClO₂ was lost in the experiments.^[67] The losses were assumed to result from partial evaporation/escape of ClO₂ during chemical addition. The initial ClO₂ dose in the simulations was adjusted according to the experimental chlorine losses.

RESULTS

Computer regression was first utilized to obtain the unknown reaction rate parameters (Kinfit software, simultaneous nonlinear curve fitting).^[81] This method

Table 4. Comparison of experimental and predicted pulp/liquor properties at time = 30 min. Experimental results are obtained from previous reports^[67,68]

Pulp	Kappa		HexA (mmol/kg)		End pH		AOX (kg/ADt)		OX (kg/ADt)	
	Exp	Pred	Exp	Pred	Exp	Pred	Exp	Pred	Exp	Pred
O-delign pulp	12.5		45							
30 kg, 45°C	6.7	7.7	22	29	3.1	3.1	0.53	0.27	0.29	0.24
20 kg, 45°C	8.0	8.2	24	32	3.3	3.2	0.51	0.22	0.27	0.20
15 kg, 45°C	8.8	8.6	29	33	3.7	3.3	0.45	0.17	0.24	0.07
20 kg, 55°C	7.9	7.7	23	31	3.1	3.1	0.43	0.24	0.25	0.19
20 kg, 65°C	7.2	7.4	24	30	3.2	3.1	0.46	0.25	0.26	0.14

was, however, found to result in severe parameter correlation. Parameter correlation often arises, when the validation data is insufficient either in amount or in quality. In our case the problems were likely to result from kappa number being the only variable used to validate a large number of competing and successive lignin oxidation reactions and AOX being the only validation variable for several organochlorine formation reactions. The reaction rate parameter tuning was eventually carried out manually. A comparison between the model prediction and experimental results is shown in Tables 4 and 5, and Figures 6–9.

The kappa number predictions coincide rather well with the experimental results. The effect of chlorine dioxide dose and temperature (Figure 6) was also estimated considerably well. A systematic deviation appeared in predicting the very rapid initial kappa drop (during the first minute): the predicted kappa number at $t = 1$ min is consistently one unit higher than the experimental value.

Table 5. Comparison of experimental and predicted oxy-chlorine concentrations at time = 30 min. Experimental data is obtained from previous papers^[67,68]

Pulp	Chlorine dioxide (mmol/l)		Chlorite (mmol/l)		Chlorate (mmol/l)		Chloride (mmol/l)	
	Exp	Pred	Exp	Pred	Exp	Pred	Exp	Pred
30 kg, 45°C	2.4	4.5	0.3	1.9	2.2	0.5	8.0	8.7
20 kg, 45°C	0.5	1.5	0.3	1.9	1.7	0.4	7.2	7.7
15 kg, 45°C	0.2	0	1.2	3.6	0.9	0.2	4.5	5.6
20 kg, 55°C	0	1.0	0.2	1.3	1.6	0.6	6.5	8.5
20 kg, 65°C	0	0.5	0	1.4	1.4	0.7	7.5	8.9

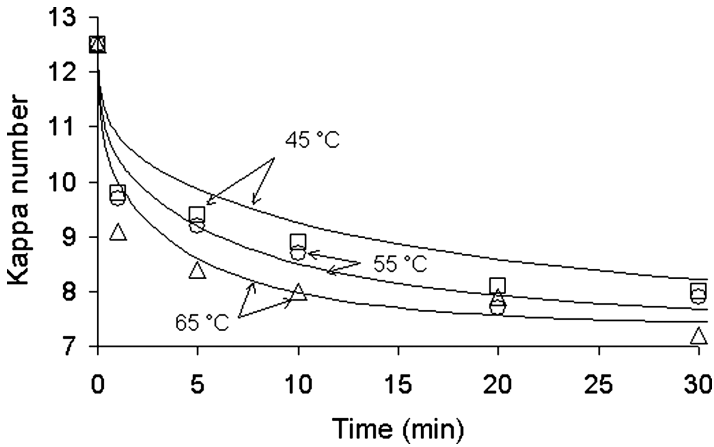


Figure 6. The predicted (line) and experimental (bullets) kappa number decrease at $T = 45^{\circ}\text{C}$, 55°C , and 65°C .

The extremely rapid initial HexA removal was well reproduced (Figure 7). The total magnitude of HexA removal was, however, systematically underestimated. The HexA removal predictions fell 3–8 mmol/kg short (Table 4, Figure 7). The effect of chemical dose on HexA removal was consistent with experiments.

The initial jump in AOX generation was well predicted (Figure 8). The following, relatively steady AOX generation (1–30 min) was, however, underestimated. The trend (intensive initial phase) of OX formation was again well predicted. The predicted effect of chemical dose on organochlorine formation (OX and AOX) was much more dramatic than observed in the experiments. Splitting the chemical dose (30 kg \rightarrow 15 kg) resulted in a 15% reduction in the

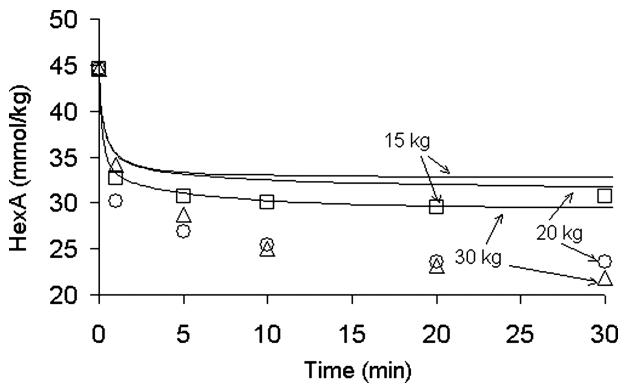


Figure 7. The predicted (line) and experimental (bullets) HexA content using 30, 20, or 15 kg act. Cl/ADt chlorine dioxide dose.

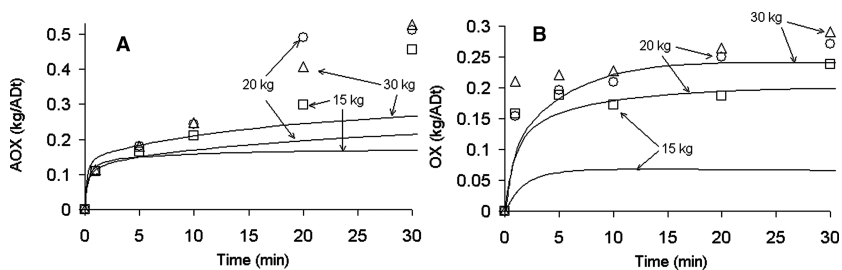


Figure 8. The predicted (line) and experimental (bullets) organochlorine formation with 30, 20, or 15 kg act. Cl/ADt chlorine dioxide dose.

final amount of AOX (t = 30 min) in the experiments. The predicted reduction was nearly 40% (Table 4). The effect of chemical dose on OX was overestimated as well. Temperature had a very small (AOX) or an insignificant (OX) effect on experimental organochlorine formation. The predicted temperature dependence on both AOX (directly proportional) and OX (inversely proportional) formation was small, yet evident.

The simulated OX consisted almost entirely of monochlorinated phenyl propane units. The amount of more extensively degraded chlorinated lignin compounds was negligible. Approximately 30% of the AOX compounds were

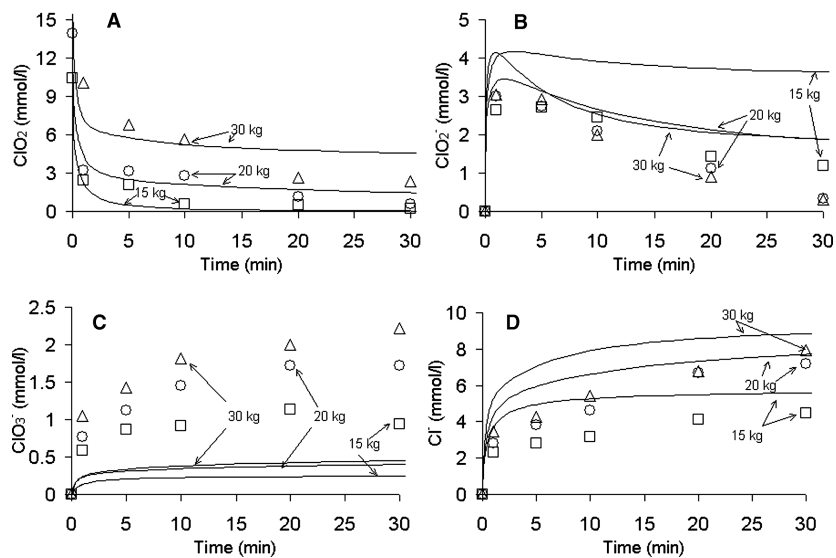


Figure 9. The predicted (line) and experimental (bullets) oxy-chlorine concentrations with 30, 20, or 15 kg act. Cl/ADt chlorine dioxide dose.

lignin related, again mainly monochlorinated phenyl propane units. The remaining part of AOX consisted of HexA degradation products. The only significant deviation from this pattern occurred with the 15 kg/ADt simulation; then only 10% of the AOX compounds were lignin related.

The chlorine dioxide consumption predictions coincided quite well with the experimental results (Figure 9A). The amount of chlorite generated within the first minute was only slightly overestimated. The depletion of chlorite toward the end of the reaction time was under-predicted, especially with in the 15 kg/ADt chemical dose simulation (Figure 9B). The trend in the predicted chlorate generation is correct, but the quantities fall severely short (Figure 9C). The simulated chloride ion concentration curves have the right shape, but the total quantity is somewhat overestimated (Figure 9D).

DISCUSSION

Kappa Number

The decrease of kappa number was in some cases slightly underestimated (Table 4). This is readily explained by the simulated HexA removal being too low. The importance of extractives (sterols and fatty acids) was found to be small regarding both the simulated kappa reduction (less than 0.5 units) and the chemical consumption. The rapid initial phase of HexA removal was well reproduced, which implies that the problems in predicting the initial kappa drop relate to modeling lignin oxidation/dissolution. The discrepancy could be explained, for instance, by lignin oxidation reactions taking place extensively on the fiber surface, so that the lignin fragments would dissolve directly into the external liquid. The model presently assumes that the lignin reactions are uniformly distributed throughout the fiber wall and the oxidized fragments need first to detach from the solid matrix (the dissolution reaction) and then diffuse out into the external liquid. Another explanation could arise from the division of lignin between phenolic (extremely reactive) and non-phenolic (very slow reaction) moieties. Although commonly used, the division may be too coarse, and in reality some structures lumped in the non-phenolic category could be consumed faster than is assumed here.

Hypochlorous Acid Driven Processes in General

Chlorine dioxide delignification involves three important processes that consume intermediately formed hypochlorous acid: HexA removal, chlorite depletion/chlorate formation, and organochlorine formation (either HOCl directly or via Cl_2). The predictions regarding each of these processes suffered from somewhat poor correlation indicating that the reactions of intermediately formed hypochlorous acid are inadequately understood. It is peculiar that the extent of

each process was underestimated; especially at reaction times 5–30 min. There was no accumulation of HOCl, so the implication is that hypochlorous acid was not being produced enough. The predictions were slightly improved, if a reaction between chlorite/chlorous acid and lignin/carbohydrate aldehydes—an additional source for HOCl—was introduced. The reaction was defined to consume chlorite/chlorous acid and to produce hypochlorous acid, while converting aldehydes into carboxylic acids.^[82,83] The aldehydes were assumed to be available in excess. Despite the slightly improved prediction, HexA removal, AOX formation, and chlorate formation were still underestimated.

Another peculiar feature is the apparent temperature independence of the hypochlorous acid driven processes. The experimental results showed that changes in temperature (45–65°C) had no effect on the rate or extent of HexA removal, OX formation, or chlorate formation. AOX formation was affected only very slightly. Hence, temperature changes had no effect on the ratio in which HOCl was consumed between the competing reaction paths. One explanation for this observation is that the initial reaction steps of each process (reactions 17–32, 37, 38, 42) have equal activation energies. Another possibility is that hypochlorous acid, when formed, reacts so rapidly that it is instantly consumed by the nearest substrate (i.e., hypochlorous acid consumption would be diffusion restricted). In this case the relative importance of the HOCl consuming processes would not be determined by reaction kinetics, but by the internal structure and distribution of substrates in the fiber wall. The simulations do not provide direct evidence to confirm this hypothesis, but the fact that hypochlorous acid concentration in the fiber bound liquid was consistently almost an order of magnitude higher than in the external liquid (diffusional restrictions *between* the liquid phases) gives additional support.

The reaction rate coefficient obtained for lignin chlorination by elemental chlorine ($k_{19} = k_{20} = 2.7 \cdot 10^4 \text{ M}^{-1}\text{s}^{-1}$ at 25°C) falls within the range reported in literature ($k_{\text{reported}} = 10^2 \dots 10^6 \text{ M}^{-1}\text{s}^{-1}$ at 25°C).^[33,36,84] The reaction rate between hypochlorous acid and hexenuronic acid ($k_{25} + k_{27} = 14 \text{ M}^{-1}\text{s}^{-1}$ at 25°C) is an order of magnitude smaller than reported for HexA model compound ($k_{\text{reported}} = 400 \text{ M}^{-1}\text{s}^{-1}$).^[85]

Organochlorine Formation

In the experiments, chemical dose had only a small effect on organochlorine formation (Table 4). The predicted effect of chemical dose was a great deal stronger (Figure 8). The effect of dose is especially large on OX, which consists exclusively of chlorinated lignin compounds (all HexA products are soluble). In the model, chlorination by elemental chlorine was assumed to be unspecific with regards to lignin, that is, the unoxidized lignin pseudo-compounds were chlorinated at equal rates (reactions 19, 20). Therefore the simulation result is logical: a higher chemical dose leads to higher quantities of hypochlorous

acid/chlorine, and consequently into more extensive chlorination. The fact that this scheme fails to predict the experimental outcome suggests that the real chlorination reactions may be specific with regard to certain lignin structures. The extent of organochlorine formation would then be dictated by the abundance of the substrates susceptible to chlorination rather than by the concentration of chlorine or hypochlorous acid. Reaction (17), the chlorination of free phenols by hypochlorous acid, is in fact an example of a structure-specific chlorination reaction. This reaction was, however, observed to be totally insignificant as the competing oxidation reactions by chlorine dioxide (reactions 1–6) were several orders of magnitude faster.

The experiments with different chemical doses also have different end pH. A higher chemical dose leads to lower pH and vice versa (Table 4). It may be that the small changes in experimental organochlorine formation may result from the changes in pH. The hypothesis of specific chlorination substrates would still give a plausible explanation for the model not being able to predict the experimental outcome.

Inorganic Chlorine Species

The simulated chlorine dioxide consumption coincided well with the experiments. The other oxy-chlorine concentrations were not predicted quite as well. The largest inconsistency appeared with chlorate formation (Figure 9C). Chlorous acid self-decomposition (reaction 35) and iron catalyzed chlorite depletion (reactions 43–49) are known to be insignificantly slow at pH above 3.^[57] The pH in our experiments was always above 3. Hence, the only mechanism leading to chlorate production is the overall reaction between hypochlorous acid and chlorous acid (reactions 37–40). Apparently, this route cannot alone account for the observed chlorate formation. It may be that some pulp related organic compounds alter the ratio of the Cl_2O_2 consuming reactions, and hence the production of chlorate.^[56,57] It may also be that oxy-chlorine radicals have a more important role than was assumed in the model.^[86,87]

The chlorite concentrations are quite well predicted at reaction times 0–10 min for the 20 and 30 kg/ADt cases (Figure 9B). At reaction time $t = 10$ –30 min the chlorite concentrations in the 20 and 30 kg/ADt experiments exhibit a steady depletion, arriving in almost complete extinction at $t = 30$ min. The predicted decay, however, slows down toward the end, leaving a notable chlorite residue. The experimental steady depletion suggests that chlorite is consumed in a reaction, where the other reactant is constantly available (pseudo-first order reaction). In the model, chlorite is consumed effectively only in reactions with hypochlorous acid and chlorine (reactions 37 and 38). Both HOCl and Cl_2 deplete rapidly in the simulations, which explains the outcome of the predictions. The 15 kg/ADt chlorite prediction shows only negligible

decay after the initial rise, leaving a major residue at $t = 30$ min. This results probably from a higher pH in the 15 kg/ADt experiment (Table 4), which shifts the equilibrium between chlorite and chlorous acid toward the former and slows down the reaction between HClO_2 and HOCl . Coherence between the predicted and experimental chlorite concentrations was reached, if a reaction between chlorous acid/chlorite and pulp related aldehydes was implemented in the model (aldehydes in excess).

The overestimation of chloride production is readily explained by simultaneous underestimations in chlorate and organochlorine formation. The chlorine balance must close, and the chlorine left over from chlorate and organochlorine formation ends up as chloride (and chlorite).

Lignin Dissolution

The predicted COD generation at $t = 30$ min ranges between 8.3 and 10.5 kgO_2/Adt . The accuracy of the COD predictions cannot be readily evaluated, since direct validation data is not available. The correlation of Jain et al.^[88] (D0-stage COD, unbleached or oxygen delignified softwood or hardwood pulp) predicts our experiments to yield COD values between 4.3 and 8.8 kgO_2/Adt (depending on the experiment). The order of magnitude is same, but the values obtained with the correlation are a bit lower. The comparison must, however, be viewed conservatively, since it does not involve direct experimental results.

CONCLUSIONS

The report introduces a model for chlorine dioxide delignification of chemical pulp. The presented model uses chemical reactions, mass transfer, and thermodynamics to describe changes in fiber and liquor composition. One of the major benefits of our approach is that it can be used to evaluate generally accepted reaction schemes. The model gave good predictions for several key variables including kappa number, chemical consumption, and pH. The effects of temperature and chemical dose were predicted right in quality, although the magnitude was overestimated. However, chlorate and organochlorine formation were under-predicted, suggesting that our present conceptions related to the reactions of intermediately formed hypochlorous acid are not satisfactory. Also, the theory of unspecific chlorination by elemental chlorine was shown to be too simple to explain the experimentally observed chemical dose dependency in organochlorine formation.

The biggest challenges in the work aroused from inability to validate the model predictions at molecular level. The experimental validation data used to characterize changes in lignin composition/content and in organochlorine formation covered standardized, structure unspecific analysis methods (kappa

number, COD, AOX, OX). Converting the molecular scale composition into these bulk variables brings an additional factor of complexity and uncertainty. The balance between model complexity and sophistication level of validation data must be borne in mind also while considering future development of the model. It would be attractive to introduce more structural lignin categories within the presently used phenolic and non-phenolic moieties, for example β -O-4-, biphenyl-, and β -5-structures. These structures would have individual reactivities and reaction patterns. The assumption of uniform lignin distribution in the fiber wall could also be replaced with a group of cell wall layers possessing a heterogeneous lignin distribution. Such modifications, however, require that suitable experimental results be available for tracking changes within the defined cell wall layers or in the various categories of lignin. Development of reliable, structure-specific analytical methods for characterizing the fiber wall and liquor components would take the value of the model onto a whole new level. It is still attractive to extend the modeling principles to cover other bleaching stages and unit operations. The chlorine dioxide reaction library could be replaced with reactions related to oxygen, hydrogen peroxide, or ozone to simulate the appropriate bleaching/delignification processes. The physico-chemical phenomena included in the model are present also in pulp washing; the main distinction appears in the presence of additional filtrate flows.

NOMENCLATURE

A	frequency factor (reaction dependent)
E_a	activation energy ($\text{J}\cdot\text{mol}^{-1}$)
c	concentration (mol/kg water or mol/kg fiber)
H	hexenuronic acid content (mmol/kg)
κ	kappa number
K	equilibrium constant (reaction dependent)
k	rate constant (reaction dependent)
L	lignin content (weight%)
M_w	molar weight (g/mol)
R	gas constant ($8.3144 \text{ J}\cdot\text{K}^{-1}\cdot\text{mol}^{-1}$)
T	temperature (K)
t	time (min)

Abbreviations

[A]	concentration of species A (M)
ADt	air dry tonne of pulp
AOX	adsorbable organic halogens
COD	chemical oxygen demand

FBL	fiber bound liquid
HMW	high molecular weight
kappa	kappa number
HexA	hexenuronic Acid
M	mol/dm ³
MA	maleic acid
NPL	non-phenolic lignin
OA	oxalic acid
OxEq	oxidation equivalent
OX	organically bound chlorine in fibers

Subscripts

arom	aromatic ring
i	component i in a list of components (i = 1..n)

REFERENCES

1. Germgard, U. Kinetics of prebleaching softwood kraft pulp with chlorine dioxide and small fractions of chlorine. *Paperi ja Puu* **1982**, *64* (2), 76–82.
2. Barroca, M.J.M.C.; Simoes, R.M.S.; Almiro, J.; Castro, A.M. Kinetics of chlorine dioxide delignification of a hardwood kraft pulp. *Appita J.* **2001**, *54* (2), 190–195.
3. Chandranupap, P.; Nguyen, K.L. Effect of pH on kinetics and bleaching efficiency of chlorine dioxide delignification. *Appita J.* **2000**, *53* (2), 441–445.
4. Savoie, M.; Tessier, P. Mathematical model for chlorine dioxide delignification. *Tappi J.* **1997**, *80* (6), 105, 112, 119, 145–153.
5. Tessier, P.; Savoie, M. Chlorine dioxide delignification kinetics and EOP extraction of softwood kraft pulp. *Can. J. Chem. Eng.* **1997**, *75* (1), 23–30.
6. Mortha, G.; Lachenal, D.; Chirat, C. In *Modeling multistage chlorine dioxide bleaching*, 11th ISWPC, Association Technique de l'Industrie Papetiere: Paris, France, 2001; 447–451.
7. Gu, Y.; Edwards, L. Virtual bleach plants, part 2: Unified ClO₂ and Cl₂ bleaching model. *Tappi J.* **2003**, *2* (7), 3–8.
8. Alén, R. Structure and chemical composition of wood. In *Papermaking Science and Technology, Book 3: Forest Products Chemistry*; Stenius, P. Eds.; Fapet Oy; Helsinki, Finland, 2000; 40.
9. Dence, C.W.; Reeve, D.W. *Pulp Bleaching: Principles and Practice*. Tappi Press: Atlanta, GA, United States, 1996; 14.
10. Helfferich, F. *Ion Exchange*; McGraw-Hill: New York, 1962.
11. Towers, M.; Scallan, A.M. Predicting the ion-exchange of kraft pulps using Donnan theory. *J. Pulp Paper Sci.* **1996**, *22* (9), J332–J337.
12. Bygrave, G.; Englezos, P. Thermodynamics-based model and data for Ca, mg, and Na ion partitioning in kraft pulp fibre suspensions. *Nordic Pulp and Paper Research J.* **2000**, *15* (2), 155–159.

13. Lindgren, J.; Wiklund, L.; Öhman, L. The contemporary distribution of cations between bleached softwood fibres and the suspension liquid, as a function of $-\text{Log}[\text{H}^+]$, ionic strength and temperature. *Nord. Pulp Paper Res. J.* **2001**, *16* (1), 24–32.
14. Räsänen, E.; Stenius, P.; Tervola, P. Model describing Donnan equilibrium, pH and complexation equilibria in fibre suspensions. *Nord. Pulp Paper Res. J.* **2001**, *16* (2), 130–139.
15. Tarvo, V.; Kuitunen, S.; Lehtimaa, T.; Tervola, P.; Räsänen, E.; Tamminen, T.; Aittamaa, J.; Vuorinen, T.; Henricson, K. Modelling of chemical pulp bleaching. *Nordic Pulp and Paper Research J.* **2008**, *23* (1), 91–101.
16. Dence, C.W.; Gupta, M.K.; Sarkanen, K.V. Studies on oxidative delignification mechanisms. II. Reactions of vanillyl alcohol with chlorine dioxide and sodium chlorite. *Tappi* **1962**, *45*, 29–38.
17. Lindgren, B.O. Chlorine dioxide and chlorite oxidations of phenols related to lignin. *Svensk Papperstidn.* **1971**, *74* (3), 57–63.
18. Ni, Y.; Shen, X.H.; van Heiningen, A.R.P. Studies on the reactions of phenolic and nonphenolic lignin model compounds with chlorine dioxide. *J. Wood Chem. Technol.* **1994**, *14* (2), 243–262.
19. Brage, C.; Eriksson, T.; Gierer, J. Reactions of chlorine dioxide with lignins in unbleached pulps. Part I. Reactions of chlorine dioxide with monomeric model compounds Representing aromatic structures in residual lignins. *Holzforschung* **1991**, *45* (1), 23–30.
20. Wajon, J.E.; Rosenblatt, D.H.; burrows, E.P. Oxidation of phenol and hydroquinone by chlorine dioxide. *Environ. Sci. Technol.* **1982**, *16* (7), 396–402.
21. Gunnarsson, N.P.-I.; Ljunggren, S.C.H. Kinetics of lignin reactions during chlorine dioxide bleaching. I: Influence of pH and temperature on the reaction of 1-(3,4-Dimethoxyphenyl) ethanol with chlorine dioxide in aqueous solution. *Acta Chem. Scand.* **1996**, *50* (5), 422–431.
22. Brage, C.; Eriksson, T.; Gierer, J. Reactions of chlorine dioxide with lignins in unbleached pulps. Part II. Reactions of chlorine dioxide with dimeric model compounds representing aromatic structures in residual lignins. *Holzforschung* **1991**, *45* (2), 147–151.
23. McKague, A.B.; Kang, G.J.; Reeve, D.W. Reactions of lignin model dimers with chlorine dioxide. *Nord. Pulp Pap. Res. J.* **1994**, *9* (2), 84–87.
24. McKague, A.B.; Reeve, D.W.; XI, F. Reaction of lignin model compounds sequentially with chlorine dioxide and sodium hydroxide. *Nord. Pulp Pap. Res. J.* **1995**, *10* (2), 114–118.
25. Brogdon, B.N.; Mancosky, D.G.; Lucia, L.A. New insights into lignin modification during chlorine dioxide bleaching sequences (I): Chlorine dioxide delignification. *J. Wood Chem. Technol.* **2004**, *24* (3), 201–219.
26. Zawadzki, M.; Runge, T.; Ragauskas, A. Facile detection of ortho- and para-quinone structures in residual kraft lignin by P31 NMR spectroscopy. *J. Pulp Pap. Sci.* **2000**, *26* (3), 102–106.
27. Lachenal, D.; Chirat, C. Improvement of ClO_2 delignification in ECF bleaching, 2000 International Pulp Bleaching Conference: Oral Presentations, June 27–30, Pulp and Paper Technical Association of Canada: Halifax, NS, Canada, 2000; 159–162.

28. Hoigne, J.; Bader, H. Kinetics of reactions of chlorine dioxide (OClO) in water—I. Rate constants for inorganic and organic compounds. *Water Res.* **1994**, *28* (1), 45–55.
29. Dence, C.W.; Reeve, D.W. *Pulp Bleaching: Principles and Practice*. Tappi Press: Atlanta, GA, United States, 1996; 127–132.
30. Kolar, J.J.; Lindgren, B.O.; Pettersson, B. Chemical reactions in chlorine dioxide stages of pulp bleaching: Intermediately formed hypochlorous acid. *Wood Sci. Technol.* **1983**, *17* (2), 117–128.
31. Ni, Y.; Kubes, G.J.; van Heiningen, A.R.P. Rate processes of chlorine species distribution during chlorine dioxide prebleaching of kraft pulp. *Nord. Pulp Paper Res. J.* **1992**, *7* (4), 200–204.
32. Yoon, B.; Wang, L.; Yoon, S.; Kim, S. Mechanism of chlorate formation in chlorine dioxide delignification. *Appita J.* **2004**, *57* (6), 472–474.
33. Soper, F.G.; Smith, G.F. Halogenation of phenols. *J. Chem. Soc.* **1926**, *6*, 1582–1591.
34. Rebenne, L.M.; Gonzalez, A.C.; Olson, T.M. Aqueous chlorination kinetics and mechanism of substituted dihydroxybenzenes. *Environ. Sci. Technol.* **1996**, *30* (7), 2235–2242.
35. Deborde, M.; von Gunten, U. Reactions of chlorine with inorganic and organic compounds during water treatment—Kinetics and mechanisms: A critical review. *Water Res.* **2008**, *42* (1–2), 13–51.
36. Voudrias, E.A.; Reinhard, M. Reactivities of hypochlorous and hypobromous acid, chlorine monoxide, hypobromous acidium ion, chlorine, bromine, and bromine chloride in electrophilic aromatic substitution reactions with p-xylene in water. *Environ. Sci. Technol.* **1988**, *22* (9), 1049–1056.
37. Ni, Y.; Kubes, G.J.; van Heiningen, A.R.P. Development of phenolic lignin during chlorine dioxide bleaching of kraft pulp. *J. Wood Chem. Technol.* **1995**, *15* (1), 153–162.
38. Joncourt, M.J.; Froment, P.; Lachenal, D.; Chirat, C. Reduction of AOX formation during chlorine dioxide bleaching. *Tappi J.* **2000**, *83* (1), 144–148.
39. Connick, R.E.; Chia, Y. The hydrolysis of chlorine and its variation with temperature. *J. Am. Chem. Soc.* **1959**, *81*, 1280–1284.
40. Ni, Y.; Kubes, G.J.; van Heiningen, A.R.P. New mechanism for pulp delignification during chlorination. *J. Pulp Paper Sci.* **1990**, *16* (1), 13–19.
41. Dahlman, O.; Reimann, A.; Ljungquist, P.; Morck, R.; Johansson, C.; Boren, H.; Grimvall, A. Characterization of chlorinated aromatic structures in high-molecular-weight BKME materials and in fulvic acids from industrially unpolluted waters. *Water Sci. Technol.* **1994**, *29* (5/6), 81–91.
42. van Buren, J.B.; Dence, C.W. Identification and estimation of primary products from the reactions of chlorine with lignin model compounds. *Tappi J.* **1967**, *50* (11), 553–560.
43. Berry, R.M.; Fleming, B.I. Why do chlorination and extraction fail to delignify unbleached kraft pulp completely? *Holzforschung* **1987**, *41* (3), 177–183.
44. Dahlman, O.; Reimann, A.; Stromberg, L.; Morck, R. High-molecular-weight effluent materials from modern ECF and TCF bleaching. *Tappi J.* **1995**, *78* (12), 99–109.

45. Vilen, E.J.; McKague, A.B.; Reeve, D.W. Quantification of muconic acid-type structures in high molecular weight material from bleach plant effluents. *Holzforchung* **2000**, *54* (3), 273–278.
46. Österberg, F.; Lindström, K. Characterization of high-molecular-mass chlorinated matter in spent bleach liquors (SBL). (2). Acidic SBL. *Holzforchung* **1985**, *39* (3), 149–158.
47. Costa, M.M.; Colodette, J.L. The impact of kappa number composition on eucalyptus kraft pulp bleachability. *Brazil. J. Chem. Eng.* **2007**, *24* (1), 61–71.
48. Juutilainen, S.; Vuorinen, T.; Vilpponen, A.; Henricson, K.; Pikka, O. Combining chlorine dioxide bleaching of birch kraft pulp with an a-stage at high temperatures, TAPPI pulping conference, Orlando, FL, USA, 31 October–4 November 1999, vol. 2; 645–651.
49. Freire, C.S.R.; Silvestre, A.J.D.; Pascoal Neto, C. Carbohydrate-derived chlorinated compounds in ECF bleaching of hardwood pulps: Formation, degradation, and contribution to AOX in a bleached kraft pulp mill. *Environ. Sci. Technol.* **2003**, *37* (4), 811–814.
50. Pascoal Neto, C.P.; Freire, C.S.R.; Silvestre, A.J.D.; Silva, A.M.S.; Evtuguin, D.V.; Cavaleiro, J.A.S. Easily degradable chlorinated compounds derived from glucuronoxylan in filtrates from chlorine dioxide bleaching of eucalyptus globulus kraft pulp. *Holzforchung* **2003**, *57* (1), 81–87.
51. Freire, C.S.R.; Silvestre, A.J.D.; Pascoal Neto, C.; Cavaleiro, J.A.S. Glucuronoxylan-derived chlorinated compounds in filtrates from chlorine dioxide bleaching: A comparative study between eucalypt (*E. Globulus*) and birch (*Betula* Spp.) kraft pulps. *Appita J.* **2004**, *57* (1), 40–42.
52. Vuorinen, T.; Fagerstrom, P.; Räsänen, E.; Vikkula, A.; Henricson, K.; Teleman, A. Selective hydrolysis of hexenuronic acid groups opens new possibilities for development of bleaching processes, 9th International Symposium on Wood and Pulping Chemistry (ISWPC), Oral Presentations, Canadian Pulp and Paper Association, (1997; M4-1–M4-4.
53. Freire, C.S.R.; Silvestre, A.J.D.; Pascoal Neto, C. Oxidized derivatives of lipophilic extractives formed during hardwood kraft pulp bleaching. *Holzforchung* **2003**, *57* (5), 503–512.
54. Jansson, M.B.; Wormald, P.; Dahlman, O. Reactions of wood extractives during ECF and TCF bleaching of kraft pulp. *Pulp and Paper Canada* **1995**, *96* (4), 42–45.
55. Björklund M.; Germgård, U.; Basta, J. Formation of AOX and OCl in ECF bleaching of birch pulp. *Tappi J.* **2004**, *3* (8), 7–11.
56. Tarvo, V.; Lehtimaa, T.; Kuitunen, S.; Vuorinen, T.; Aittamaa, J. The kinetics and stoichiometry of the reaction between hypochlorous acid and chlorous acid in mildly acidic solutions. *Ind. Eng. Chem. Res.* **2009**, *48* (13), 6280–6286.
57. Tarvo, V.; Lehtimaa, T.; Kuitunen, S.; Alopaeus, V.; Vuorinen, T. Chlorate formation in chlorine dioxide delignification—An analysis via elementary kinetic modelling. *J. Wood Chem. Technol.* **2009**, *29* (3), 191–213.
58. Lehtimaa, T.; Tarvo, V.; Mortha, G.; Kuitunen, S.; Vuorinen, T. The reactions and kinetics of Cl(III) decomposition. *Ind. Eng. Chem. Res.* **2008**, *47* (15), 5284–5290.

59. Gordon, G.; Kieffer, R.G.; Rosenblatt, D.H. The chemistry of chlorine dioxide. *Prog. Inorg. Chem.* **1972**, *15*, 201–286.
60. von, Heijne, G.; Teder, A. Kinetics of the decomposition of aqueous chlorine dioxide solutions. *Acta Chem. Scand.* **1973**, *27* (10), 4018–4019.
61. Svenson, D.R.; Kadla, J.F.; Chang, H.; Jameel, H. Effect of pH on the inorganic species involved in a chlorine dioxide reaction system. *Ind Eng Chem Res* **2002**, *41* (24), 5927–5933.
62. Germgard, U.; Teder, A.; Tormund, D. Chlorate formation during chlorine dioxide bleaching of softwood kraft pulp. *Paperi Puu* **1981**, *63* (3), 127–133.
63. Norgren, M.; Lindström, B. Dissociation of phenolic groups in kraft lignin at elevated temperatures. *Holzforschung* **2000**, *54* (5), 519–527.
64. Ragnar, M.; Lindgren, C.T.; Nilvebrant, N. pK_a-values of guaiacyl and syringyl phenols related to lignin. *J. Wood Chem. Technol.* **2000**, *20* (3), 277–305.
65. Dean, J.A., Ed.; *In Lange's Handbook of Chemistry*; McGraw-Hill Inc.: New York, USA, 1999.
66. Teleman, A.; Harjunpaa, V.; Tenkanen, M.; Buchert, J.; Hausalo, T.; Drakenberg, T.; Vuorinen, T. Characterisation of 4-Deoxy-*Beta*-L-*Threo*-Hex-4-Enopyrano syluronic acid attached to xylan in pine kraft pulp and pulping liquor by ¹H and ¹³C NMR spectroscopy. *Carbohydr. Res.* **1995**, *272* (1), 55–71.
67. Lehtimaa, T.; Tarvo, V.; Kuitunen, S.; Jääskeläinen, A.-S.; Vuorinen, T. The effect of process variables in chlorine dioxide prebleaching of birch kraft pulp. Part 2. AOX and OX formation. *J. Wood Chem. Technol.* **2010**, *30* (1), 19–30.
68. Lehtimaa, T.; Tarvo, V.; Kuitunen, S.; Jääskeläinen, A.-S.; Vuorinen, T. The effect of process variables in chlorine dioxide prebleaching of birch kraft pulp. Part 1. Inorganic chlorine compounds, kappa number, lignin and hexenuronic acid content. *J. Wood Chem. Technol.* **2010**, *30* (1), 1–18.
69. Kyrklund, B.; Strandell, G. Applicability of the chlorine number for evaluation of the lignin content of pulp. *Pap. Puu (Pap. Timber)* **1969**, *51* (4a), 299–305.
70. Li, J.; Gellerstedt, G. The contribution to kappa number from hexenuronic acid groups in pulp xylan. *Carbohydr. Res.* **1997**, *302* (3–4), 213–218.
71. Li, J.; Gellerstedt, G. On the structural significance of the kappa number measurement. *Nord. Pulp Paper Res. J.* **1998**, *13* (2), 153–158.
72. Brogdon, B.N. Influence of oxidized lignin structures from chlorine dioxide delignified pulps on the kappa number test. *J. Pulp Paper Sci.* **2001**, *27* (11), 364–369.
73. Li, J.; Sevastyanova, O.; Gellerstedt, G. The relationship between kappa number and oxidizable structures in bleached kraft pulps. *J. Pulp Paper Sci.* **2002**, *28* (8), 262–266.
74. Hamzeh, Y. Evaluation De Nouveaux Procédés de Delignification et Blanchement en Réacteur a Déplacement de Liqueur, et Comparaison avec les Procédés Traditionnels, Ph.D. Thesis, EFPG, Grenoble, France, 2005.
75. Jakobsson, K.; Aittamaa, J. Introduction to Flowbat Software; <http://www.tkk.fi/Units/ChemEng/research/Software/flowbat/index.html> (accessed June 2009).
76. Alén, R. Structure and chemical composition of wood. In *Papermaking Science and Technology, Book 3: Forest Products Chemistry*. Stenius, P. Eds.; Fapet Oy; Helsinki, Finland, 2000; 40.
77. Räsänen, E.; Kärkkäinen, L. Modelling of complexation of metal ions in pulp suspensions. *J. Pulp Paper Sci.* **2003**, *29* (6), 196–203.

78. Räsänen, E. Modelling ion exchange and flow in pulp suspension, Ph.D. Thesis, VTT Processes, Espoo, Finland, 2003.
79. Laine, J.; Buchert, J.; Viikari, L.; Stenius, P. Characterization of unbleached kraft pulps by enzymatic treatment, potentiometric titration, and polyelectrolyte adsorption. *Holzforschung* **1996**, *50* (3), 208–214.
80. Lehtimaa, T. Uuteaineiden käyttäytyminen koivusulfaattisellun valmistuksessa, M.Sc. Thesis, HUT, Espoo, Finland, 2003; 99 p.
81. Jakobsson, K.; Aittamaa, J. KINFIT User's Manual; http://www.tkk.fi/Units/ChemEng/research/Software/kinfit/KINFIT_eng.html (accessed June 2009).
82. Jiang, Z.-H.; van Lierop, B.; Berry, R. Improving chlorine dioxide bleaching with aldehydes. *J. Pulp Paper Sci.* **2007**, *33* (2), 89–94.
83. Lehtimaa, T.; Tarvo, V.; Mortha, G.; Vuorinen, T. The role of chlorite in chlorine dioxide bleaching, Proceedings from the 14th ISWFPC, TAPPSA: Durban, SA, 2007.
84. Grimley, E.; Gordon, G. Kinetics and mechanism of the reaction between chlorine and phenol in acidic aqueous solution. *J. Phys. Chem.* **1973**, *77* (8), 973–978.
85. Adorjan, I.; Jääskeläinen, A.-S.; Vuorinen, T. Synthesis and characterization of the hexenuronic model methyl 4-deoxy-b-L-*thero*-hex-4-enopyranosiduronic acid. *Carboh. Res.* **2006**, *341* (14), 138–141.
86. Lindgren, B.O.; Nilsson, T. Chlorate formation during reaction of chlorine dioxide with lignin model compounds. *Svensk Papperstidning–Nordisk Cellulosa* **1975**, *78* (2), 66–68.
87. Kolar, J.J.; Lindgren, B.O. Oxidation of styrene by chlorine dioxide and by chlorite in aqueous solutions. *Acta Chem. Scand.* **1982**, *36 B* (9), 599–605.
88. Jain, S.; Mortha, G.; Calais, C. New predictive models for COD from all stages in full ECF bleaching sequences, UKSim 10th International Conference on Computer Modelling and Simulation, EUROSIM/UKSim2008, Institute of Electrical and Electronics Engineers Computer Society: Cambridge, United Kingdom, 2008; 278–283.
89. Aieta, E.M.; Roberts, P.V. Kinetics of the reaction between molecular chlorine and chlorite in aqueous solution. *Environ.Sci.Technol.* **1986**, *20* (1), 50–55.
90. Wang, T.X.; Margerum, D.W. Kinetics of reversible chlorine hydrolysis: Temperature dependence and general-acid/base-assisted mechanisms. *Inorg. Chem.* **1994**, *33* (6), 1050–1055.
91. Schmitz, G.; Rooze, H. Reaction mechanism for chlorite and chlorine dioxide. 3. Disproportionation of chlorite. *Can. J. Chem.* **1985**, *63* (4), 975–980.

APPENDIX: REACTION LIBRARY FOR THE CHLORINE DIOXIDE DELIGNIFICATION MODEL

The temperature dependency of reaction rate coefficients is modeled with the Arrhenius equation (A1), where A_r and $E_{a,r}$ are the reaction specific frequency factor and activation energy, respectively, R is the molar gas constant, and T is temperature in Kelvins.

$$k_r = A_r \cdot \exp(-E_{a,r}/R \cdot T) \quad (\text{A1})$$

Reactions between Oxy-Chlorine Species and Organic Substrates

The rate equations for reactions (1–34) are of first order with respect to the inorganic chlorine species (ClO_2 , HOCl , Cl_2) and the organic substrate. For instance, the rate of reaction (1) is:

$$\text{reaction rate}_1 = -\frac{d[\text{ClO}_2]}{dt} = k_{1,\text{undiss}} \cdot [\text{ClO}_2] \cdot [\text{phenol}] + k_{1,\text{diss}} \cdot [\text{ClO}_2] \cdot [\text{phenolate}]$$

where

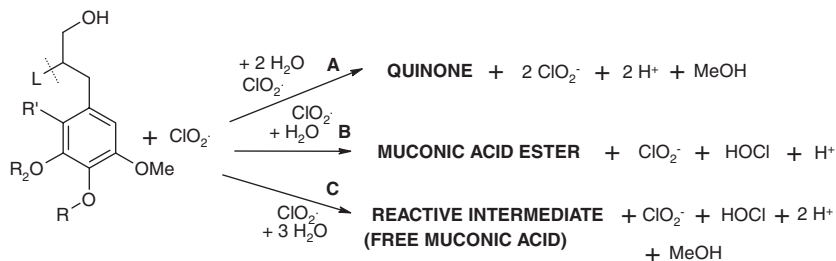
$k_{1,\text{undiss}}$ = reaction rate coefficient (1) regarding the undissociated phenol
 $k_{1,\text{diss}}$ = reaction rate coefficient (1) regarding the dissociated phenol (phenolate)

The form of the rate equation requires that all species concentrations be given in volume based molar units (mol/l). The molar concentrations (mol/l) of the solid fiber wall components were determined by dividing the mass based fiber wall contents (mol/kg fibers) with the volume of the fiber bound liquid (l/kg fibers).

Reactions (1–24) apply for lignin structures in fiber wall and in liquor (fiber bound liquid and external liquid).

Chlorine Dioxide and Lignin

Reactions (1–24) represent lignin oxidation and chlorination reactions. The reaction stoichiometric equations are introduced within the text and the reaction rate parameters are given in Tables A1–A4.



Reactions (1–3) represent the parallel paths of phenolic lignin oxidation by chlorine dioxide. The combined rates of reactions (1–3) ($1 \cdot 10^9 \text{ M}^{-1} \text{ s}^{-1}$ for the dissociated form and $1 \cdot 10^3 \text{ M}^{-1} \text{ s}^{-1}$ for the undissociated form) equal the values reported by Hoigne and Bader.^[28] The same principle applies for reactions (4–6)

Table A1. Rate parameters for oxidation of unreacted lignin by chlorine dioxide

Reaction	Route	R	R'	k/(M ⁻¹ s ⁻¹) at 25°C		E _a /(kJ mol ⁻¹)
				Undissociated	Dissociated	
1	A	-H	-H	250 ^[28]	2.5·10 ⁸	52 ^[28]
2	B	-H	-H	250 ^[28]	2.5·10 ⁸	52 ^[28]
3	C	-H	-H	500 ^[28]	5·10 ⁸	52 ^[28]
4	A	-lignin	-H	1.5·10 ⁻⁴ ^[19]	—	52
5	B	-lignin	-H	1.5·10 ⁻⁴ ^[19]	—	52
6	C	-lignin	-H	3·10 ⁻⁴ ^[19]	—	52
7	A	-H	-Cl	25	2.5·10 ⁷	52
8	B	-H	-Cl	25	2.5·10 ⁷	52
9	C	-H	-Cl	50	5·10 ⁷	52
10	A	-lignin	-Cl	<i>1.5·10⁻⁵</i>	—	52
11	B	-lignin	-Cl	<i>1.5·10⁻⁵</i>	—	52
12	C	-lignin	-Cl	<i>3·10⁻⁵</i>	—	52

Parameter values typed in italic were obtained in this work.

and the value reported by Brage et al.^[19] The rates of reactions (7–12), the respective oxidation reactions of mono-chlorinated lignin pseudo-compounds, are adjusted to an order of magnitude lower level than their unchlorinated counterparts.

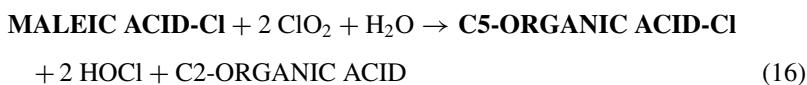
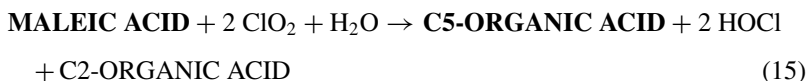
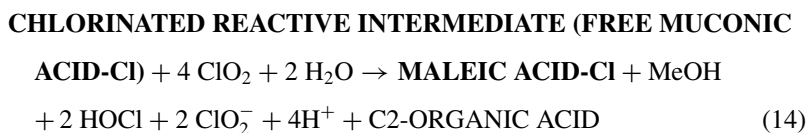
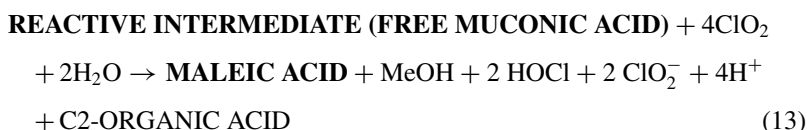


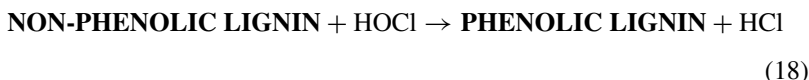
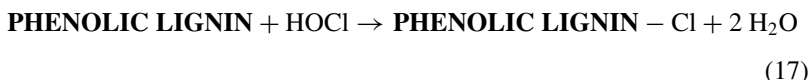
Table A2. Rate parameters for oxidation of lignin derivatives by chlorine dioxide

Reaction	$k/(M^{-1}s^{-1})$ at 25°C	$E_a/(kJ\ mol^{-1})^a$
11	<i>1.4</i>	52
12	<i>0.14</i>	52
13	<i>0.077</i>	52
14	<i>0.0077</i>	52

^aAll lignin oxidation reactions by chlorine dioxide are assumed to possess the same activation energy.

All parameters were obtained in this work.

Reactions between Hypochlorous Acid and Lignin Derivatives

**Table A3.** Rate parameters for reactions between hypochlorous acid and lignin

Reaction	k at 25°C ($M^{-1}s^{-1}$)		E_a ($kJ\ mol^{-1}$)
	Undissociated	Dissociated	
17	<i>0.36^[35]</i>	<i>$2.7 \cdot 10^4$^[35]</i>	<i>41.5</i>
18	<i>2.7</i>	—	<i>41.5</i>

Parameters typed in italic were obtained in this work.

Reactions between Chlorine and Lignin Derivatives

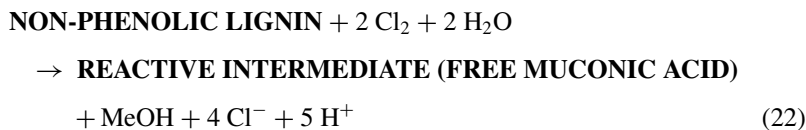
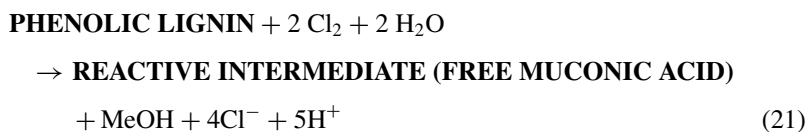
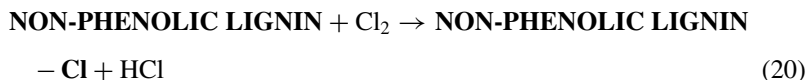




Table A4. Rate parameters for reactions between elemental chlorine and lignin

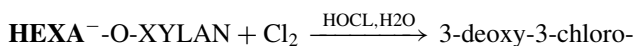
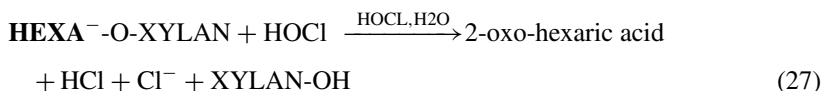
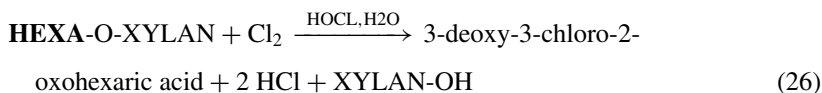
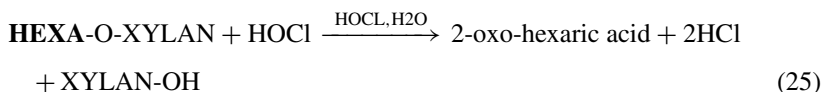
Reaction	k at 25°C (M ⁻¹ s ⁻¹)	E _a (kJ mol ⁻¹)
19	2700 ^a	41.5
20	2700	41.5
21	270 ^a	41.5
22	270	41.5
23	27 ^a	41.5
24	27	41.5

^aThe undissociated and dissociated forms of phenols are assumed to react at equal rates.

All rate parameters were obtained in this work.

Reactions between HOCl/Cl₂ and Hexenuronic Acid + Derivatives

Hexenuronic acid exists only in the fiber wall. All HexA reactions (25–28) lead to breakage of the chemical bond that attaches HexA to xylan. The primary reaction products of HexA (2-oxo-hexaric acid and 3-deoxy-3-chloro-2-oxohexaric acid) are assumed to be dissolved in the fiber bound liquid immediately. The subsequent reactions (28–32) take place in the fiber bound and external liquid. The stoichiometric equations for the HexA related reactions (25–32) are introduced below. The related reaction rate parameters are provided in Table A5.



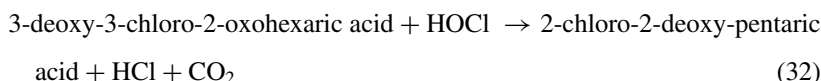
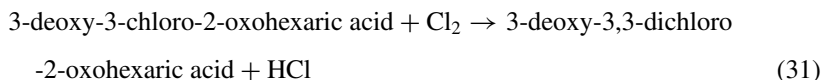
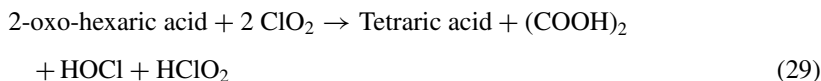


Table A5. Rate parameters for the HexA reactions

Reaction	k at 25°C (M ⁻¹ s ⁻¹)	E _a (kJ mol ⁻¹)
25	6.9	41.5
26	540	41.5
27	6.9	41.5
28	540	41.5
29	1400	41.5
30	700	41.5
31	1.5·10 ⁴	41.5
32	560	41.5

All rate parameters were obtained in this work.

Chlorine Dioxide and Extractives

Both the unreacted and oxidized extractives exist only in the fiber wall (no dissolution). Reactions (33) and (34) represent the oxidation of extractives by chlorine dioxide. The appropriate reaction rate parameters are given in Table A6.

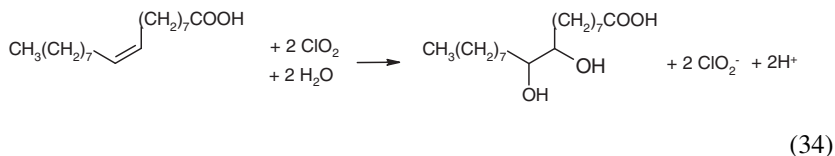
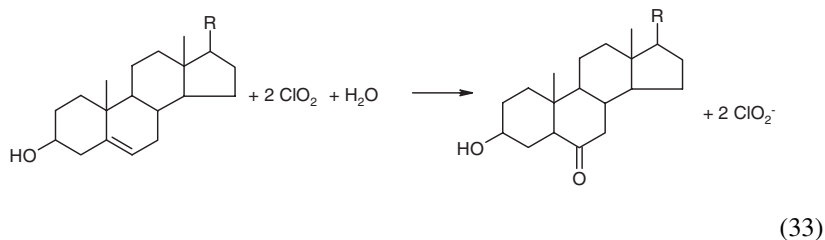


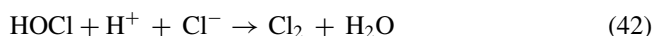
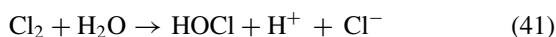
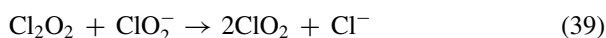
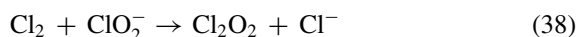
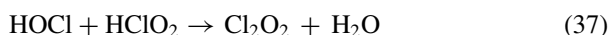
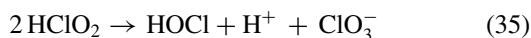
Table A6. Rate parameters for reactions between chlorine dioxide and extractives

Reaction	k at 25°C (M ⁻¹ s ⁻¹)	E _a (kJ mol ⁻¹)
33	10	56
34	10	56

All rate parameters were obtained in this work.

Inorganic Oxy-Chlorine Reactions

Reactions (35–49) represent the fully inorganic oxy–chlorine reactions. The appropriate reaction rate parameters are given in Table A7.



Iron Catalysed Chlorite Decomposition

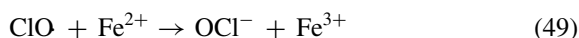
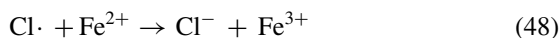
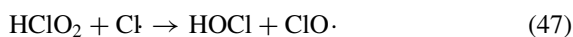
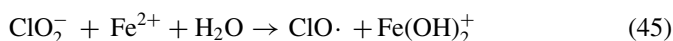
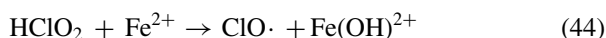
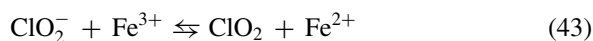


Table A7. Rate parameters for the inorganic oxy-chlorine reactions

Reaction	k at 25°C (M ⁻¹ s ⁻¹)	E _a (kJ·mol ⁻¹)	Reference
35	0.0021 M ⁻¹ s ⁻¹	81	[58]
36	0.0027 M ⁻² s ⁻¹	67	[58]
37	406 M ⁻¹ s ⁻¹	54	[56]
38	9.1·10 ³ M ⁻¹ s ⁻¹	39.9	[89]
39	8.4·10 ⁹ ·[Cl ⁻] M ⁻² s ⁻¹	50	[56]
40	5.3·10 ⁵ M ⁻¹ s ⁻¹	78	[56]
41	6.4 s ⁻¹	63	[90]
42	1.3·10 ⁴ M ⁻² s ⁻¹	31	[90]
43	k ₄₃ = 269 M ⁻¹ s ⁻¹	95	[91]
	k _{43, rev} = 4.7·10 ⁵ M ⁻¹ s ⁻¹	95	[57]
44	930 M ⁻¹ s ⁻¹	95	[91]
45	530 M ⁻¹ s ⁻¹	95	[57]
46/49	k ₄₆ /k ₄₉ = 2.2·10 ⁻⁴	—	[57]
47/48	k ₄₇ /k ₄₈ = very small	—	[57]

rev = reverse (rate coefficient for the reverse reaction).

Equilibrium Reactions

The equilibrium reactions incorporated in the model (50–65) are listed below. The related equilibrium coefficients (K_a) of pK_a-values are given in Tables A8 and A9.

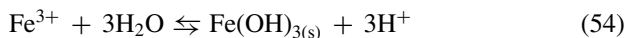
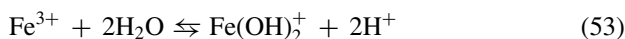
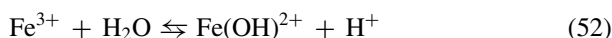
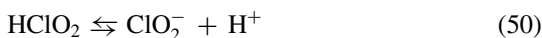


Table A8. Equilibrium coefficients for the inorganic equilibrium reactions

Reaction	Equilibrium coefficient (at 25°C)
50	K _{a,50} = 0.019 M
51	K _{a,51} = 2.28 · 10 ⁻⁸ M
52	K ₅₂ = 6.5 · 10 ⁻³ M
53	K ₅₃ = 4.9 · 10 ⁻⁷ M ²
54	K ₅₄ = 1.6 · 10 ⁻³⁹ M ²

All coefficient values (temperature dependency included) are computed from thermochemical constants.^[15,65]

Table A9. Equilibrium coefficients for protolysis reactions of organic pseudo-compounds

Reaction	Protolysis description	pK _a -value (at 25°C)	Reference
55	Phenolic lignin protolysis constant	^a pK _a = 10.4	[63]
56	Chlorinated Phenolic lignin protolysis constant	^a pK _a = 9.4	[28]
57 and 58	Muconic acid protolysis constants	^b pK _{a,1} = 2.2; ^b pK _{a,2} = 4.4	Lehtimaa et al., unpublished results
59 and 60	Maleic acid protolysis constants	^b pK _{a,1} = 1.9; ^b pK _{a,2} = 6.3	[65]
61	C-5 aliphatic acid protolysis constant	^b pK _a = 3	assumed value
62 and 63	Oxalic acid protolysis constants	^b pK _{a,1} = 1.2; ^b pK _{a,2} = 4.2	[65]
64	HexA protolysis constant	^c pK _a = 3.0	[66]
65	Glucuronic acid protolysis constant	^c pK _a = 3.1	[66]

^aTemperature dependency adopted from a value reported for kraft lignin phenols.^[63]

^bThe value is assumed to be temperature independent.

^cTemperature dependency is estimated using the enthalpy of dissociation (−3 kJ/mol) reported for uronic acids in kraft pulp fibers.^[13]

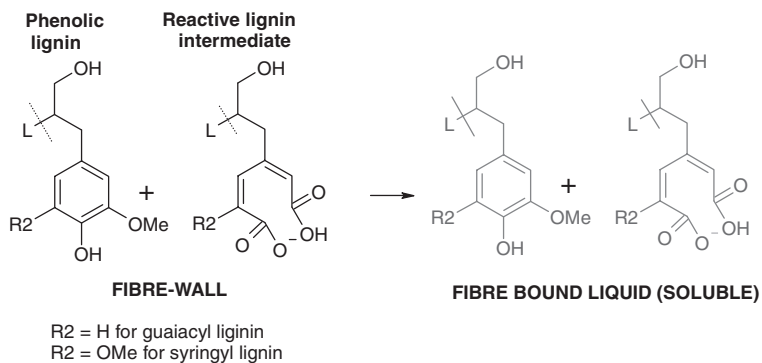
Lignin Dissolution Reactions

All lignin dissolution reactions are assigned the same rate parameters:

$$k_i = 8.7 \cdot 10^{-3} \text{ M}^{-1} \text{ s}^{-1} \quad (i = 66 - 101)$$

$$E_{a,i} = 50 \text{ kJ/mol} \quad (i = 66 - 101)$$

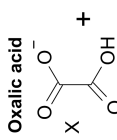
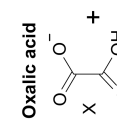
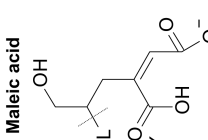
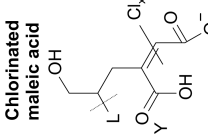
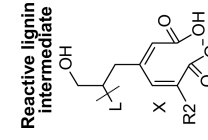
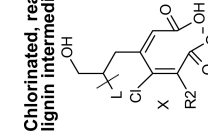
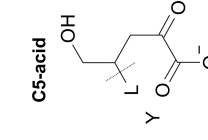
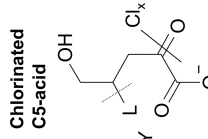
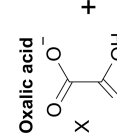
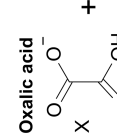
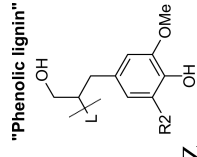
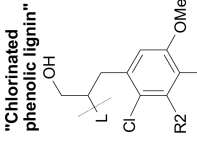
The parameter values were obtained from regression. The principle of higher lignin degradation and hydrophilicity leading to more extensive dissolution is achieved through differences in dissolution stoichiometry. The dissolution stoichiometries are given in Table A10. Each cell in the table defines a stoichiometry and reaction order for one reaction: X, Y, and Z (capital letters) give the stoichiometric coefficients, and x, y, and z (small letters) indicate the order of the reaction rate with regards to each participating compound. For instance the leftmost cell on the top row defines that “reactive lignin intermediate” and phenolic lignin dissolve in reaction (66) in a 1:1 ratio and the reaction rate is first order with regards to both compounds. The scientific notation for the reaction stoichiometry and rate is shown in Scheme A1.

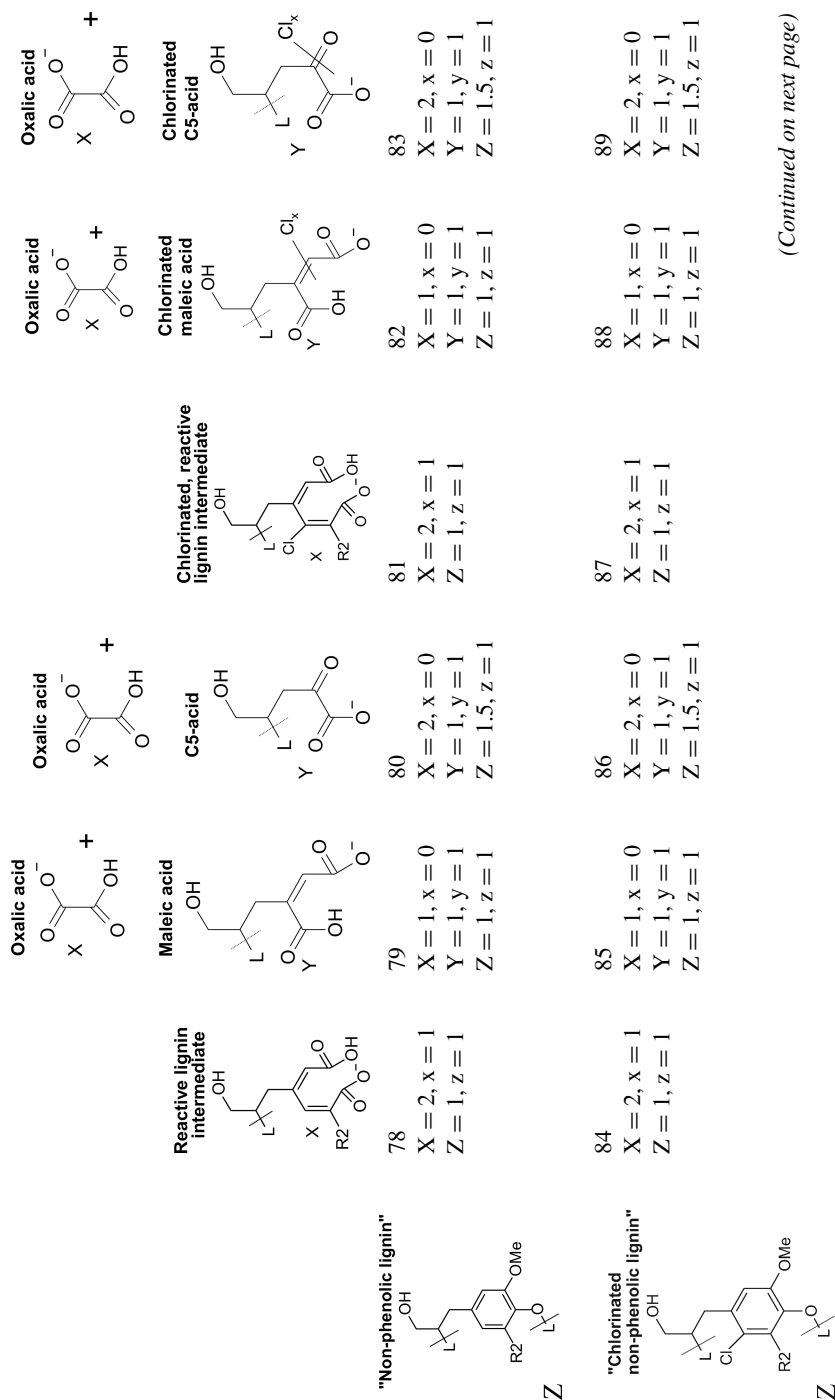


$$\text{reaction rate} = k \cdot [\text{phenolic lignin}]_{\text{FIBER}} \cdot [\text{reactive lignin intermediate}]_{\text{FIBER}}$$

Scheme A1. An example of a lignin dissolution reaction.

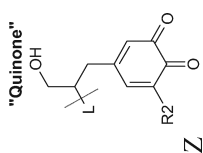
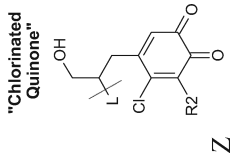
Table A10. The stoichiometric and rate matrix for lignin dissolution reactions. The capital letters (X, Y, Z) represent stoichiometric coefficients and small letters (x, y, z) indicate the reaction order with regards to each participating compound

Fragmented and hydrophilic lignin pseudo-compounds	
<p>Oxalic acid</p>  <p>Oxalic acid</p>	<p>Oxalic acid</p>  <p>Oxalic acid</p>
<p>Maleic acid</p>  <p>Maleic acid</p>	<p>Chlorinated maleic acid</p>  <p>Chlorinated maleic acid</p>
<p>Reactive lignin intermediate</p>  <p>Reactive lignin intermediate</p>	<p>Chlorinated, reactive lignin intermediate</p>  <p>Chlorinated, reactive lignin intermediate</p>
<p>C5-acid</p>  <p>C5-acid</p>	<p>Chlorinated C5-acid</p>  <p>Chlorinated C5-acid</p>
<p>Oxalic acid</p>  <p>Oxalic acid</p>	<p>Oxalic acid</p>  <p>Oxalic acid</p>
Unfragmented lignin pseudo-compounds	
<p>"Phenolic lignin"</p>  <p>"Phenolic lignin"</p>	<p>66 X = 2, x = 1 Z = 1, z = 1</p>
<p>"Chlorinated phenolic lignin"</p>  <p>"Chlorinated phenolic lignin"</p>	<p>72 X = 2, x = 1 Z = 1, z = 1</p>
<p>67 X = 1, x = 0 Y = 1, y = 1 Z = 1, z = 1</p>	<p>68 X = 2, x = 0 Y = 1, y = 1 Z = 1.5, z = 1</p>
<p>69 X = 2, x = 1 Z = 1, z = 1</p>	<p>70 X = 1, x = 0 Y = 1, y = 1 Z = 1, z = 1</p>
<p>71 X = 2, x = 0 Y = 1, y = 1 Z = 1.5, z = 1</p>	<p>73 X = 1, x = 0 Y = 1, y = 1 Z = 1, z = 1</p>
<p>74 X = 2, x = 0 Y = 1, y = 1 Z = 1.5, z = 1</p>	<p>75 X = 2, x = 1 Z = 1, z = 1</p>
<p>76 X = 1, x = 0 Y = 1, y = 1 Z = 1, z = 1</p>	<p>77 X = 2, x = 0 Y = 1, y = 1 Z = 1.5, z = 1</p>



(Continued on next page)

Table A10. The stoichiometric and rate matrix for lignin dissolution reactions. The capital letters (X, Y, Z) represent stoichiometric coefficients and small letters (x, y, z) indicate the reaction order with regards to each participating compound (*Continued*)

		Fragmented and hydrophilic lignin pseudo-compounds										
 "Quinone" Z	90	X = 2, x = 1 Y = 1, z = 1	91	X = 1, x = 0 Y = 1, y = 1 Z = 1, z = 1	92	X = 2, x = 0 Y = 1, y = 1 Z = 1.5, z = 1	93	X = 2, x = 1 Z = 1, z = 1	94	X = 1, x = 0 Y = 1, y = 1 Z = 1, z = 1	95	X = 2, x = 0 Y = 1, y = 1 Z = 1.5, z = 1
	 "Chlorinated Quinone" Z	96	X = 2, x = 1 Z = 1, z = 1	97	X = 1, x = 0 Y = 1, y = 1 Z = 1, z = 1	98	X = 2, x = 0 Y = 1, y = 1 Z = 1.5, z = 1	99	X = 2, x = 1 Z = 1, z = 1	100	X = 1, x = 0 Y = 1, y = 1 Z = 1, z = 1	101

R2 = H for guaiacyl lignin, R2 = OMe for syringyl lignin.